MODELING ON RAYLEIGH SCATTERING IN OPTICAL WAVEGUIDES

A THESIS SUBMITTED TO
THE GRADUATE SCHOOL OF NATURAL AND APPLIED SCIENCES
OF
THE MIDDLE EAST TECHNICAL UNIVERSITY

BY

BURAK ÇAMAK

IN PARTIAL FULFILLMENT OF REQUIREMENTS FOR THE DEGREE OF
MASTER OF SCIENCE
IN
THE DEPARTMENT OF PHYSICS

SEPTEMBER 2003

Approval of the Graduate School of Natural and Applied Sciences.

Prof. Dr. Canan ÖZGEN
Director

I certify that this thesis satisfies all the requirements as a thesis for the Degree of Master of Science.

Prof. Dr. Sinan BİLİKMEN
Head of the Department

This is to certify that we read this thesis and that in our opinion it is fully adequate, in scope and quality, as a thesis for degree of Master of Science.

Assoc. Prof. Dr. Serhat ÇAKIR
Supervisor

Examining Committee Members

Prof. Dr. Sinan BİLİKMEN _____

Assoc. Prof. Dr. Akif ESENDEMİR _____

Assoc. Prof. Dr. Gülay ÖKE _____

Dr. Ali ALAÇAKIR _____

Assoc. Prof. Dr. Serhat ÇAKIR _____

ABSTRACT

MODELING ON RAYLEIGH SCATTERING IN OPTICAL WAVEGUIDES

Çamak, Burak

M.Sc., Department of Physics

Supervisor: Assoc. Prof. Dr. Serhat Çakır

September 2003, 83 pages

In the last few years, interest in polymer optical fibers (POF) has increased because of their low cost, easy handling and good flexibility even at large diameters. Moreover, optical cables do not have the problem of electromagnetic interference, which gives, for instance, the problem of cross-talk in copper telephone cables. In the usage of current communication and computer systems the yield has gained a big importance and it has seen from studies that light scattering loss is the only loss, which cannot be eliminated entirely. Besides, this loss causes its attenuation loss intrinsically and determines the lower limit of loss in the POF.

In this work, the importance and the dependencies of light scattering were studied, and calculations were done in order to find more appropriate polymer for using as core material of POFs. For this aim, a computer program that calculates the light scattering loss of several amorphous polymers and plots the graph of isotropic scattering loss

versus isothermal compressibility and total attenuation loss versus wavelength was written.

Key Words: Rayleigh Scattering, Light Scattering, Isothermal Compressibility, Plastic Optical Fibers.

ÖZ

OPTİK DALGA KLAVUZLARINDA RAYLEIGH SAÇILMASI ÜZERİNE MODELLEME

Çamak, Burak
Yüksek Lisans, Fizik Bölümü
Tez Yöneticisi: Doç. Dr. Serhat Çakır

Eylül 2003, 83 sayfa

Son birkaç yıl içerisinde, ucuz maliyeti, kolay kablolanması ve esnekliği polimer optik fiberlere (POF) olan ilgiyi arttırmıştır. Ayrıca, optik kablolarda, bakır telefon kablolarındaki cross-talk problemi gibi elektromanyetik girişim problemi de yoktur. Şu an kullanılan iletişim ve bilgisayar sistemlerinde ürün büyük bir önem kazanmıştır ve araştırmalardan görülmektedir ki; ışık saçılmasından dolayı oluşan kayıp tamamen ortadan kaldırılamayan tek kayıptır ve bu kayıp POF' taki kaybın alt limitini de belirler.

Bu çalışmada, ışık saçılımının önemi ve bağlı olduğu parametreler incelendi ve plastik optik fiberlerin çekirdek maddesi olarak kullanılacak en uygun polimeri bulmak için hesaplamalar yapıldı. Bu amaçla, farklı polimerler için ışık saçılımı kayıplarını hesaplayan, izotropik saçılma / eşısı sıkıştırılabilirliği ve toplam zayıflama kaybı / dalga boyu grafiklerini çizen bir program yazıldı.

Anahtar Kelimeler: Rayleigh Saçılması, Işık Saçılması, Eşısı Sıkıştırılabilirliği, Plastik Optik Fiber.

ACKNOWLEDGEMENTS

I would like to express sincere appreciation to my supervisor Assoc. Prof. Dr. Serhat Çakır for his guidance, discussions, encouragement, and excellent patience during this thesis.

I am also grateful to my friend, Pınar and Musa for their helps and suggestion.

I would also like to thank to my wife Alev and my colleagues for their supports and encouragements.

TABLE OF CONTENTS

LIST OF TABLES

TABLE

LIST OF FIGURES

FIGURES

CHAPTER 1

INTRODUCTION

1.1 General Background

For current communication and computer systems there is a demand for high-volume data transfer. Copper wires cannot satisfy this need because of low transmission speed and small signal bandwidth (information-carrying capacity). Information transmission by using optical cables, which transport pulses of light instead of electricity, increases bandwidth with a factor 1,000. Compared to telephone cable it is even a factor up to 10,000 [1].

The cost for each polymer optical fiber (POF) connection is approximately 1/100th the cost of a glass fiber connection. This is because polymers are more flexible than glass and so POF can be manufactured with larger diameters. Also, polymers allow for a wide range of refractive indices, which means that POF can be designed with a larger numerical aperture (NA) compared to the NA of glass fiber. Larger diameter fiber and NA translate into less stringent requirements for alignment and therefore lower cost for each connection. POF has been demonstrated to achieve high-bandwidth (>2 GHz.km) [2].

Moreover, signal attenuation is considerably lower for optical systems and thus transmission distance can be much larger without the need for signal boosting. Furthermore, optical cables do not have the problem of electromagnetic interference, which gives, for instance, the problem of cross-talk in copper telephone cables.

Silicate glass is the most transparent material known and optical glass fibers with extremely low attenuation of light transmission and high bandwidth have been developed in the past decades. These optical glass fibers have been used for long distance telecommunications. The basic configuration of an optical fiber and some important characteristics are shown in Fig. 1.1.

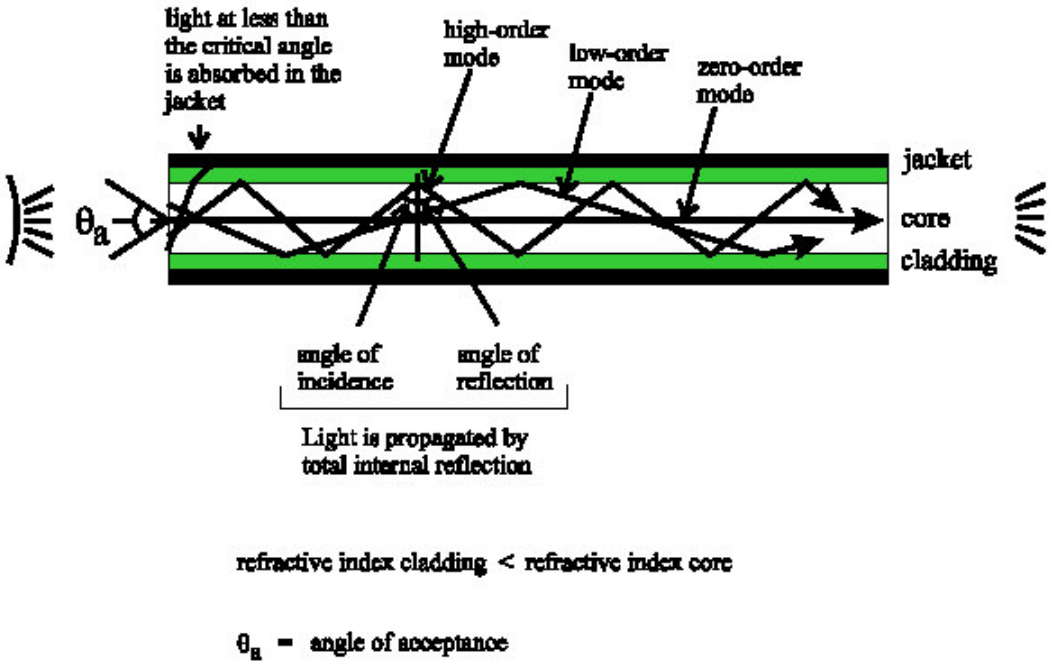

Figure 1.1 Depiction of an optical fiber [1].

Although optical fiber appears to be only a simple thread, it is actually composed two structures. The area where light is transmitted is called the core, and the external area is called the clad. Light can be transmitted through transparent media by means of total

internal reflection, which is possible in a core-cladding configuration. The cladding must have a lower refractive index than the core. Fig. 1.1 and Fig. 1.2 shows a step-index optical fiber, which means that the refractive index is constant along the fiber core cross-section and immediately changes (step-wise) to the refractive index of the cladding.

Light rays propagate via discrete paths through a fiber. Each distinct path is called a mode and corresponds to a certain angle of incidence. Consequently, different modes take different times to travel along the fiber. The total number of light modes which can be coupled in is defined by the numerical aperture (NA). The NA is limited by the refractive index difference between cladding and core. The NA is thereby directly related to the angle of acceptance and the latter is given by the formula:

$$NA = (n_1^2 - n_2^2)^{1/2} = n_0 \sin(\theta_a/2) \tag{1.1}$$

where n_0, n_1 and n_2 are refractive indices of outer medium (usually, n = 1), the core and the cladding respectively.

The larger the difference in refractive index, the higher is the number of modes, which can be guided through the fiber. In a step-index fiber, the number of possible modes N_m of wavelength λ is related to NA and the fiber diameter (d) following Eq.(1.2).

$$N_m = 0.5\left(\frac{\pi d NA}{\lambda}\right)^2 \tag{1.2}$$

In the situation that only one mode is available for the light rays, the fiber is called single-mode. Single-mode fibers are prepared by reducing the core diameter to dimensions well below the wavelength of the light used. Larger cores can accept more light modes and these fibers are, therefore, called multi-mode.

Step-index multi mode optical fiber (SI-MMF) has relatively wide core and refractive indices of both core and cladding are constant. In SI-MMF, the propagation light can be guided by total internal reflection on the surface of core and cladding. Total internal reflection is the phenomena that all incoming light energy is reflected back into the incident medium for incident angles greater than or equal to the critical angle.

In the SI optical fiber, differences in optical path length depending on incident angle are large. Therefore, SI optical fiber has many optical modes.

All polymer based optical fibers commercially developed so far are of a multimode step-index (SI) type, where a homogeneous core with higher refractive index is sheathed in cladding material with lower refractive index, and their attenuation is 100-300dB/km. Step-index plastic optical fibers can be manufactured by means of a melt spinning process such as coaxial extrusion. In the case of the SI fiber, with an increase in the core diameter, the transmission bandwidth decreases due to its modal dispersion and the input pulses become broader through the fiber. Therefore, even in a short distance optical communication, the plastic SI fiber cannot cover the whole bandwidth over hundreds of MHz which will be necessary for the fast datalink and LANs in the near future.

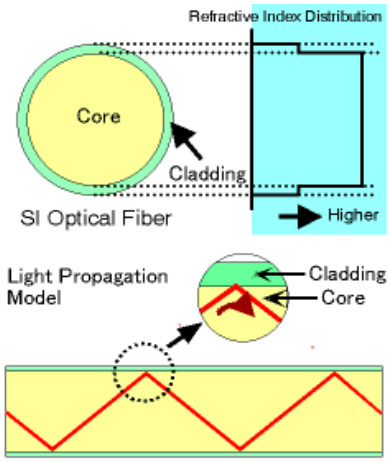

Figure 1.2 Step index optical fiber [10].

Another possibility is a graded-index fiber, for which the refractive index gradually increases from a high value in the center toward a lower value at the perimeter of the core. Therefore, it utilizes the principle of refraction, not reflection as in the previous example.

This method is the same as what occurs when light refracts at the surface of water. GI fiber uses this principle to progressively change the track of the light to contain it within the fiber. Multi step structure fiber uses the both of the above principles for transmission. As its name indicates, the structure uses multiple step indexes.

Although the basic principle is the same as that of SI-POF, because the index of refraction changes in multiple steps, the locus of the light is shifted toward the center at the same time.

Also, since it can easily be applied to varying bandwidths by changing the number of steps, it has the added benefit of simple conversion to larger capacities in the future.

Graded-index (GI) plastic optical fibers, whose refractive index distribution is expressed in Eq.(1.3), is expected to have a much higher bandwidth than the SI fibers, regardless of a large diameter.

$$n(r) = n_0\left(1 - \frac{1}{2}Ar^2\right) \tag{1.3}$$

where, n_0 and $n(r)$ are the refractive indices at the center axis and r is the distance from the center and A is the distribution constant.

Because of modal dispersion, the difference of optical paths of light, step-index plastic optical fibers have a bandwidth of hundreds of MHz. It cannot be used in the high-speed data network. But the modal dispersion of graded-index plastic optical fiber is much

smaller than that of step-index optical fiber. Because its bandwidth is much higher than 3 GHz, graded index plastic optical fiber can be used in the short distance data network [3].

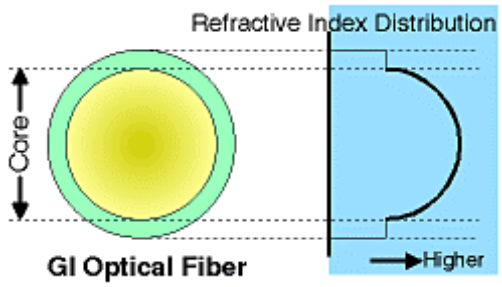

Figure 1.3 Graded index optical fiber [11].

The information-carrying capacity of optical fibers is largely determined by the level of signal dispersion and the refractive index profile along the core cross-section. Clearly, the initial modulation of light determines the starting pulse width and the pulse frequency and thus directly the bandwidth of the total system. However, most important for the bandwidth is the level of signal dispersion in the optical fiber. Through signal dispersion, pulses of light start to interfere (overlap of pulses), meaning that information will be lost and the bandwidth will thereby be reduced. The bandwidth is given in bits.km/s or in Hz.km. Signal dispersion is caused by modal, material and waveguide dispersion. Modal dispersion is the dominant factor and is caused by the different path lengths traveled by light modes with different angles of incidence (see Fig. 1.1). The fastest mode is the zero-order mode traveling straight through the center of the fiber core. In single-mode fibers only the zero-order mode is accepted and such fibers have the highest bandwidth (100 GHz.km) possible. However, such fibers have extremely small core diameters. The bandwidth of step-index multi-mode fibers is about 10 MHz.km. To increase the transmission rate, graded-index fibers with low signal dispersion have been developed. Such fibers can have bandwidths of more than 2 GHz.km, still possessing large core diameters (0.5 – 1.0 mm). In graded-index fibers the light spirals through the fiber core. Light travels faster in lower refractive index material.

Light modes with a high angle of acceptance have to travel longer distances, but spend most of the time in lower refractive index material, thereby going faster. For light modes with a smaller angle of acceptance the opposite is true. The overall effect is a reduced pulse broadening with respect to step-index fibers.

Glass optical fibers have small core diameters ranging from a few micrometers for single-mode up to 100 – 125 micrometers for multi-mode fibers. Such small core diameters are necessary due to the brittleness of glass. Only with small core diameters do these fibers have some flexibility at room temperature. To protect such a weak core material, several extra layers are necessary, making fiber production costly. The major drawback of such small core diameters, however, is in the coupling of fibers. Minute core-to-core shifts quickly result in high coupling losses. Although this is well understood, connector design is difficult and costly. A further disadvantage of glass optical fibers is their low numerical aperture (NA $\approx$ 0.16), which complicates coupling even more. The difficult and costly coupling process is the reason that glass optical fibers are not used for local area networks or computer networks, for which lots of connections have to be realized.

Recently there has been considerable interest in the development of polymer optical fibers (POFs). The ductility of polymers is an important advantage and confers on POFs easy processing, easy handling, low costs and large core diameter. POFs have an extended applicability, e.g. in computer networks, local area networks, datalinks, optical sensors, lighting, etc. The large core diameter, up to 1 mm or more, enables high efficiencies of fiber coupling. Furthermore, because polymers have low densities they are light-weight. Transmission of light occurs with wavelengths from the visible part of the spectrum (550 - 850 nm), because of the presence of low-loss windows in this particular region.

Disadvantages of current POFs are high optical losses and low thermal resistance. Transmission loss is, besides bandwidth, the most important parameter determining the

usefulness of an optical fiber. It is expressed in decibels (dB) and measured by using a cut-off method.

1.2 Attenuation and Rayleigh Scattering

As an optical signal propagates through a material, it will be degraded by attenuation and dispersion. Dispersion can sometimes be compensated or eliminated through clever design, but attenuation simply leads to a loss of signal. Eventually the energy in the signal becomes so weak that it cannot be distinguished with sufficient reliability from the noise always present in the system. Attenuation therefore determines the maximum distance that optical links can be operated without amplification [4].

The attenuation of a fiber is then defined as the logarithm of the ratio between output intensities of the two different fiber lengths and normalized over the length of the fiber cut-off:

$$Attenuation(\alpha) = \frac{10}{L}\log(\frac{I_2}{I_1}) \tag{1.4}$$

L is the length of fiber cut-off, I_2 is the outgoing light intensity after cutting off a length L and I_1 the outgoing intensity before cutting.

For a polymer to be transparent it has to be fully amorphous. Polymers which meet this requirement and are applied for POFs are, for instance, poly(methyl methacrylate) (PMMA), poly(styrene) (PS), poly(carbonate) (PC) and poly(siloxane) rubber. Worldwide, research and development have been predominantly focused on PMMA. Transmission losses of commercial PMMA-based POFs are typically 100 - 200 dB/km (100 dB/km means a transmission distance of 200 m if one assumes a technical detection limit of 1% of the initial light intensity). Attenuation of the signal in POFs is caused by

various mechanisms. The different contributions to the total loss mechanism can be divided into intrinsic and extrinsic losses. The individual contributions are tabulated in Tab. 1.1.

Intrinsic losses are related to the molecular structure of the plastic core material, while the extrinsic losses can be minimized by purification and optimization of the processing. Intrinsic absorption losses are caused by the higher harmonics of molecular vibrations in the IR-region and electronic transitions in the UV-region. In addition to these intrinsic absorption phenomena, which are determined by the medium material itself, absorption by contaminants, such as transition metals and organic impurities can play a role. They are classified as extrinsic absorptions, in the sense that they are not a property of the polymer, but depend mainly on manufacturing conditions (purification).

Intrinsic Losses		Extrinsic Losses	
Absorption	Scattering	Absorption	Scattering
Higher harmonics of C-H vibration	Rayleigh scattering	Transition metals	Dust and microvoids
Electronic transition $\pi - \pi^*, \sigma - n$		Organic contaminants	Core diameter fluctuations
			Orientational birefringence
			Core-cladding boundary imperfections

Table 1.1 The individual contributions to the total loss mechanism of polymer optical fibers [1].

Rayleigh scattering in dielectrics arises from small density fluctuations that are frozen into the dielectric during manufacture and composition and by anisotropy of polarizability. When an optical fiber is formed, the glass is pulled through an oven, where the molten material is stretched to become a thin fiber. After leaving the oven it freezes back into an amorphous solid. There is a high level of thermal agitation at the transition temperature (melting point) of glass, and this thermodynamical disorder leads to compositional and density fluctuations. These random variances are frozen in, and serve as the source for subsequent Rayleigh scattering. This is a fundamental process: there is nothing that can be done to eliminate the thermal agitation that accompanies melting thermal material for manufacture of waveguides.

This form of scattering is intrinsic for a certain polymer and is mainly important in the UV-region of the spectrum, because it is inversely proportional to the fourth power of the wavelength of the scattered radiation (Eq.(1.5)). It has been shown that Rayleigh scattering is predominantly caused by fluctuations in density. Eq.(1.5) gives the intensity of light scattering due to fluctuations in density and anisotropy of polarizability (τ_d):

$$\tau_d = C\frac{8\pi^3}{3\lambda_0^4}\left(\frac{(n^2-1)(n^2+2)}{3}\right)^2 kT_g\beta \qquad (1.5)$$

where C is Cabannes factor, λ_0 is the wavelength in vacuum, n is the refractive index, k is Boltzmann's constant, T_g is the glass transition temperature and β is the isothermal compressibility.

From materials point of view, a low refractive index and small compressibility favor reduction of scattering due to density fluctuations. The Cabannes factor corrects for the molecular anisotropy. To illustrate the latter, PS has a Cabannes factor of 2.7 that for PMMA is 1.1

Consequently it can be understood that attenuation arises from several different physical effects. In an optical waveguide, one must consider 1) intrinsic material absorptions, 2) absorptions due to impurities, 3) Rayleigh scattering (light scattering), 4) bending and waveguide scattering losses, and 5) microbending loss. In terms of priority, Rayleigh scattering is the most serious causes of power loss for long-distance systems in optical waveguides. Taking into consideration all these reasons mentioned above, the importance and the dependencies of intrinsic light scattering loss will be studied in this thesis.

CHAPTER 2

LIGHT SCATTERING AND ATTENUATION THEORY

2.1 Scattering by Dipoles Induced in Small Scatterers

The scattering of electromagnetic waves by systems whose individual dimensions are small compared with a wavelength is a common and important occurrence. In such interactions it is convenient to think to the incident (radiation) field as inducing electric and magnetic multipoles that oscillate in definite phase relationship with the incident wave and radiate energy in directions other than the direction of incidence. The exact form of the angular distribution of radiated energy is governed by the coherent superposition of multipoles induced by the incident fields and in general depends on the state of polarization of the incident wave. If the wavelength of the radiation is long compared to the size of the scatterer, only the lowest multipoles, usually electric and magnetic dipoles, are important [5].

The customary basic situation is for a plane monochromatic wave to be incident on a scatterer. For simplicity the surrounding medium is taken to have $\mu_r = \varepsilon_r = 1$. If the incident direction is defined by the unit vector $\hat{n}_0$, and the incident polarization vector is $\hat{\varepsilon}_0$, the incident fields are

$$\vec{E}_{inc} = \hat{\varepsilon}_0 E_0 e^{ikn_0 \cdot x}$$
$$\vec{H}_{inc} = \hat{n}_0 \times \vec{E}_{inc} / Z_0 \tag{2.1}$$

where $k = \omega/c$ and a time-dependence $e^{-i\omega t}$ is understood. These fields induce dipole moments $\vec{p}$ and $\vec{m}$ in the small scatterer and these dipoles radiate energy in all directions. Far away from the scatterer, the scattered (radiated) fields are

$$\vec{E}_{sc} = \frac{1}{4\pi\varepsilon_0} k^2 \frac{e^{ikr}}{r} \left[(\hat{n} \times \vec{p}) \times \hat{n} - \hat{n} \times \vec{m}/c \right]$$
$$\vec{H}_{sc} = \hat{n} \times \vec{E}_{sc} / Z_0 \tag{2.2}$$

where $\hat{n}$ is a unit vector in the directions of observation and r is the distance away from the scatterer. The power radiated in the direction $\hat{n}$ with polarization ε, per unit solid angle, per unit incident flux (power per unit area) in the direction $\hat{n}_0$ with polarization $\hat{\varepsilon}_0$, is a quantity with dimensions of area per unit solid angle. It is called the differential scattering cross section:

$$\frac{d\sigma}{d\Omega}(n, \varepsilon; n_0, \varepsilon_0) = \frac{r^2 \frac{1}{2Z_0} \left| \hat{\varepsilon}^* \cdot \vec{E}_{sc} \right|^2}{\frac{1}{2Z_0} \left| \hat{\varepsilon}_0^* \cdot \vec{E}_{inc} \right|^2} \tag{2.3}$$

The complex conjugation of the polarization vectors in Eq.(2.3) is important for the correct handling of circular polarization. With Eq.(2.2) and Eq.(2.1), the differential cross section can be written

$$\frac{d\sigma}{d\Omega}(n, \varepsilon; n_0, \varepsilon_0) = \frac{k^4}{(4\pi\varepsilon_0 E_0)^2} \left| \hat{\varepsilon}^* \cdot \vec{p} + (\hat{n} \times \hat{\varepsilon}^*) \cdot \vec{m}/c \right|^2 \tag{2.4}$$

The dependence of the cross section on $\hat{n}_0$ and $\hat{\varepsilon}_0$ is implicitly contained in the dipole moments $\vec{p}$ and $\vec{m}$. The variation of the differential (and total) scattering cross section with wave number as k^4 (or in wavelength as λ^{-4}) is an almost universal characteristic of the scattering of long-wavelength radiation by any finite system. This dependence on frequency is known as Rayleigh's law. Only if both static dipole moments vanish does the scattering fail to obey Rayleigh's law; the scattering is then via quadrupole or higher multipoles (or frequency-dependent dipole moments) and varies as ω^6 or higher. Sometimes the dipole scattering is known as Rayleigh scattering, but this term is usually reserved for incoherent scattering by a collection of dipole scatterers.

2.2 Perturbation Theory of Scattering, Scattering by Gases and Liquids, Attenuation in Optical Fibers

2.2.1 General Theory

If the medium through which an electromagnetic wave is passing is uniform in its properties, the wave propagates undisturbed and undeflected. If, however, there are spatial (or temporal) variations in the electromagnetic properties, the wave is scattered. Some of the energy is deviated from its original course. If the variations in the properties are small in magnitude, the scattering is slight and perturbative methods can be employed. We imagine a comparison situation corresponding to a uniform isotropic medium with electric permittivity ε_0 and magnetic permeability μ_0. For the present ε_0 and μ_0 are assumed independent of frequency, although when harmonic time dependence is assumed this restriction can be removed in the obvious way. Through the action of some perturbing agent, the medium is supposed to have small changes in its response to applied fields, so that $D \neq \varepsilon_0 E$, $B \neq \mu_0 H$, over certain regions of space. These departures may be functions of time and space variables. Beginning with the Maxwell equations in the absence of sources [5],

$$\vec{\nabla}\cdot\vec{B}=0, \qquad \vec{\nabla}\times\vec{E}=-\frac{\partial\vec{B}}{\partial t}$$

$$\vec{\nabla}\cdot\vec{D}=0, \qquad \vec{\nabla}\times\vec{H}=\frac{\partial\vec{D}}{\partial t} \tag{2.5}$$

it is a straightforward matter to arrive at a wave equation for D,

$$\nabla^2\vec{D}-\mu_0\varepsilon_0\frac{\partial^2\vec{D}}{\partial t^2}=-\vec{\nabla}\times\vec{\nabla}\times(\vec{D}-\varepsilon_0\vec{E})+\varepsilon_0\frac{\partial}{\partial t}\vec{\nabla}\times(\vec{B}-\mu_0\vec{H}) \tag{2.6}$$

It is convenient to specialize to harmonic time variation with frequency ω for the unperturbed fields and to assume that the departures $(\vec{D}-\varepsilon_0\vec{E})$ and $(\vec{B}-\mu_0\vec{H})$ also have this time variation. This puts certain limitations on the kind of perturbed problem that can be described by the formalism, but prevents the discussion from becoming too involved. With a time dependence $e^{-i\omega t}$ understood, Eq.(2.6) becomes

$$(\nabla^2+k^2)\vec{D}=-\vec{\nabla}\times\vec{\nabla}\times(\vec{D}-\varepsilon_0\vec{E})-i\varepsilon_0\omega\vec{\nabla}\times(\vec{B}-\mu_0\vec{H}) \tag{2.7}$$

where $k^2=\mu_0\varepsilon_0\omega^2$, and μ_0 and ε_0 can be values specific to the frequency ω. The solution of the unperturbed problem, with the right-hand side of Eq.(2.7) set equal to zero, will be denoted by $\vec{D}^{(0)}(x)$. Thus

$$\vec{D}=\vec{D}^{(0)}+\frac{1}{4\pi}\int d^3x'\frac{e^{ik|x-x'|}}{|x-x'|}\left\{\vec{\nabla}'\times\vec{\nabla}'\times(\vec{D}-\varepsilon_0\vec{E})+i\varepsilon_0\omega\vec{\nabla}'\times(\vec{B}-\mu_0\vec{H})\right\} \tag{2.8}$$

If the physical situation is one of scattering, with the integrant in Eq.(2.8) confined to some finite region of space and $\vec{D}^{(0)}$ describing a wave incident in some direction, the field far away from the scattering region can be written as

$$\vec{D} \to \vec{D}^{(0)} + \vec{A}_{sc} \frac{e^{ikr}}{r} \tag{2.9}$$

where the scattering amplitude $\vec{A}_{sc}$ is

$$\vec{A}_{sc} = \frac{1}{4\pi} \int d^3x' e^{-ikn\cdot x'} \left\{ \vec{\nabla}' \times \vec{\nabla}' \times (\vec{D} - \varepsilon_0 \vec{E}) + i\varepsilon_0 \omega \vec{\nabla}' \times (\vec{B} - \mu_0 \vec{H}) \right\} \tag{2.10}$$

Some integrations by parts in Eq.(2.10) allow the scattering amplitude to be expressed as

$$\vec{A}_{sc} = \frac{k^2}{4\pi} \int d^3x e^{-ikn\cdot x} \left\{ \left[\hat{n} \times (\vec{D} - \varepsilon_0 \vec{E}) \right] \times \hat{n} - \frac{\varepsilon_0 \omega}{k} \hat{n} \times (\vec{B} - \mu_0 \vec{H}) \right\} \tag{2.11}$$

The vectorial structure of the integrant can be compared with the scattered dipole field Eq.(2.2). the polarization dependence of the contribution from $(\vec{D} - \varepsilon_0 \vec{E})$ is that of an electric dipole, from $(\vec{B} - \mu_0 \vec{H})$ a magnetic dipole. In correspondence with Eq.(2.4) the differential scattering cross section is

$$\frac{d\sigma}{d\Omega} = \frac{\left| \hat{\varepsilon}^* \cdot \vec{A}_{sc} \right|^2}{\left| \vec{D}^{(0)} \right|^2} \tag{2.12}$$

where ε is the polarization vector of the scattered radiation.

Eq.(2.8), Eq.(2.11), and Eq.(2.12) provide a formal solution to the scattering problem. The scattering amplitude $\vec{A}_{sc}$ is not known, of course, until the fields are known at least approximately. But from Eq.(2.8) a symmetric scheme of successive approximations can be developed in the same way as the Born approximation series of quantum-mechanical scattering. If the integrand in Eq.(2.8) can be approximated to first order, then Eq.(2.8)

provides a first approximation for $\vec{D}$, beyond $\vec{D}^{(0)}$. This approximation to $\vec{D}$ can be used to give a second approximation for the integrand, and an improved $\vec{D}$ can be determined, and so on.

2.2.2 Born Approximation

We will be content with the lowest order approximation for the scattering amplitude. This is called the first Born approximation or just the Born approximation in quantum theory and was actually developed in the present context by Lord Rayleigh in 1881. Furthermore, we shall restrict our discussion to the simple example of spatial variations in the linear response of the medium. Thus we assume that the connections between $\vec{D}$ and $\vec{E}$ and $\vec{B}$ and $\vec{H}$ are

$$\begin{aligned} \vec{D}(x) &= [\varepsilon_0 + \delta\varepsilon(x)]\vec{E}(x) \\ \vec{B}(x) &= [\mu_0 + \delta\mu(x)]\vec{H}(x) \end{aligned} \tag{2.13}$$

where $\delta\varepsilon(x)$ and $\delta\mu(x)$ are small in magnitude compared with ε_0 and μ_0. The differences appearing in Eq.(2.8) and Eq.(2.11) are proportional to $\delta\varepsilon$ and $\delta\mu$. To lowest order then, the fields in these differences can be approximated by the unperturbed fields:

$$\begin{aligned} \vec{D} - \varepsilon_0\vec{E} &\cong \frac{\delta\varepsilon(x)}{\varepsilon_0}\vec{D}^{(0)}(x) \\ \vec{B} - \mu_0\vec{H} &\cong \frac{\delta\mu(x)}{\mu_0}\vec{B}^{(0)}(x) \end{aligned} \tag{2.14}$$

If the unperturbed fields are those of a plane wave propagating in a direction $\hat{n}_0$, so that $\vec{D}^{(0)}$ and $\vec{B}^{(0)}$ are

$$\vec{D}^{(0)}(x) = \varepsilon_0 D_0 e^{ikn_0 \cdot x}$$

$$\vec{B}^{(0)}(x) = \sqrt{\frac{\mu_0}{\varepsilon_0}} n_0 \times \vec{D}^{(0)}(x)$$

the scalar product of the scattering amplitude Eq.(2.11) and $\hat{\varepsilon}^*$, divided by D_0, is

$$\frac{\hat{\varepsilon}^* \cdot \vec{A}_{sc}^{(1)}}{D_0} = \frac{k^2}{4\pi} \int d^3x e^{iq \cdot x} \left\{ \hat{\varepsilon}^* \cdot \hat{\varepsilon}_0 \frac{\delta\varepsilon(x)}{\varepsilon_0} + (\hat{n} \times \hat{\varepsilon}^*) \cdot (\hat{n}_0 \times \hat{\varepsilon}_0) \frac{\delta\mu(x)}{\mu_0} \right\} \tag{2.15}$$

where $q = k(n_0 - n)$ is the difference of the incident and scattered wave vectors. The absolute square of Eq.(2.15) gives the differential scattering cross section Eq.(2.12).

If the wavelength is large compared with the spatial extent of $\delta\varepsilon$ and $\delta\mu$, the exponential in Eq.(2.15) can be set equal to unity. The amplitude is then a dipole approximation analogous to the preceding section, with the dipole frequency dependence and angular distribution.

2.2.3 Density Fluctuations; Critical Opalescence

An alternative and more general approach to the scattering and attenuation of light in gasses and liquids is to consider fluctuations in the density and so the index of refraction. The volume V of fluid is imagined to be divided into cells small compared to a wavelength, but each containing very many molecules. Each cell has volume v with an average number $N_v = vN$ of molecules inside. The actual number of molecules fluctuates around N_v in a manner that depends on the properties of the gas or liquid. Let the departure from the mean of the number of molecules in the *j*th cell be ΔN_j. The variation in index of refraction $\delta\varepsilon$ for the *j*th cell is

$$\delta\varepsilon_j = \frac{\partial\varepsilon}{\partial N}\frac{\Delta N_j}{v}$$

From the Clausius-Mossotti relation, this can be written

$$\delta\varepsilon_j = \frac{(\varepsilon_r - 1)(\varepsilon_r + 2)}{3Nv}\Delta N_j \tag{2.16}$$

With this expression for the $\delta\varepsilon$ for the *j*th cell, the integral Eq.(2.15), now a sum over cells, becomes

$$\frac{\hat{\varepsilon}^* \cdot \vec{A}_{sc}^{(1)}}{D_0} = \varepsilon^* \cdot \varepsilon_0 \frac{k^2(\varepsilon_r - 1)(\varepsilon_r + 2)}{12\pi N\varepsilon_r}\sum_j \Delta N_j e^{iq\cdot x_j} \tag{2.17}$$

In forming the absolute square of Eq.(2.17) a structure factor similar to $\vec{F}(q) = \left|\sum_j e^{iq\cdot x_j}\right|^2$ will occur. If it is assumed that the correlation of fluctuations in different cells (caused indirectly by the intermolecular forces) only extends over a distance small compared to a wavelength, the exponential in Eq.(2.17) can be put equal to unity. Then the extinction coefficient α, given by

$$\alpha = \frac{1}{V}\int\left|\frac{\varepsilon^* \cdot \vec{A}_{sc}^{(1)}}{D_0}\right|^2 d\Omega$$

is

$$\alpha = \frac{(\omega/c)^4}{6\pi N}\left|\frac{(\varepsilon_r - 1)(\varepsilon_r + 2)}{3}\right|^2 \cdot \frac{\Delta N_v^2}{NV} \tag{2.18}$$

where ΔN_v^2 is the mean square number fluctuation in the volume V, defined by

$$\Delta N_v^2 = \sum_{jj'} \Delta N_j \Delta N_{j'}$$

the sum being over all the cells in the volume V. With the use of statistical mechanics the quantity ΔN_v^2 can be expressed in terms of the isothermal compressibility β_T of the medium:

$$\frac{\Delta N_v^2}{NV} = NkT\beta_T, \qquad \beta_T = -\frac{1}{V}\left(\frac{\partial V}{\partial P}\right)_T \tag{2.19}$$

The attenuation coefficient Eq.(2.18) then becomes

$$\alpha = \frac{1}{6\pi N}\left(\frac{\omega}{c}\right)^4 \left|\frac{(\varepsilon_r - 1)(\varepsilon_r + 2)}{3}\right|^2 \cdot NkT\beta_T \tag{2.20}$$

This particular expression, first obtained by Einstein in 1910, is called the Einstein-Smoluchowski formula. For a dilute ideal gas, with $|\varepsilon - 1| << 1$ and $NkT\beta_T = 1$, it reduces to the Rayleigh result ($\alpha = N\sigma \cong \frac{2k^4}{3\pi N}|n-1|^2$). As the critical point is approached, β_T becomes very large (infinite exactly at the critical point). The scattering and attenuation thus become large there. This is the phenomenon known as critical opalescence. The large scattering is directly related to the large fluctuations in density near the critical point. Very near the critical point our treatment so far fails because the correlation length for the density fluctuations becomes greater than a wavelength.

2.2.4 Attenuation in Optical Fibers

It is of interest that the ultimate limiting factor setting the maximum distance between repeater units in optical fiber transmission is the unavoidable attenuation caused by

Rayleigh scattering, and by infrared absorption at longer wavelengths. The isothermal compressibility of silica glass is $\beta_T \approx 7\times10^{-11}\ \ m^2/N$, while the relevant temperature $T \approx 1400K$ (called the fictive temperature) is where the fluctuations are frozen in (approximately the annealing temperature). The effective value of $(\varepsilon_r - 1)(\varepsilon_r + 2)/3 \approx 1.30\,in$ in Eq.(2.20) is somewhat smaller than the 1.51 inferred from an index of refraction of $n = 1.45$ at $\lambda = 1.0\,\mu m$. The net result is that $\alpha\,(km^{-1}) \approx 0.2/[\lambda\,(\mu m)]^4$. The conversion to decibels per kilometer (a factor of 4.343) gives $\alpha\,(dB/km) \approx 0.85/[\lambda(\mu m)]^4$. For wavelengths less than $1.5\mu m$, the attenuation is dominated by Rayleigh scattering, plus the absorption by impurities such as the hydroxyl ions from very small amounts of water dissolved in the glass. At wavelengths longer than $1.6\,\mu m$, infrared absorption sets in strongly. The minimum attenuation of about $0.2\,db/km$ occurs at $\lambda \approx 1.55\,\mu m$. The absorption mean free path at the minimum is $22\ km$.

CHAPTER 3

EMPIRICAL PREDICTION METHOD OF INTRINSIC LIGHT SCATTERING LOSS OF TRANSPARENT AMORPHOUS POLYMERS

In the last few years, interest in polymer optical fibers (POFs) has increased because of their low cost, easy handling and good flexibility even at large diameters. They are easier to connect each other and to light sources because of their large core diameter and high numerical aperture (NA). The development of POFs leads to the fundamental question about the transmission loss limit of amorphous polymer glasses. The two important intrinsic loss factors in POFs are molecular vibration absorption and scattering due to fluctuation. The molecular vibration absorption loss can be calculated from molecular structure by using Morse potential theory, and the fluctuation theory indicates that the isotropic light scattering loss of amorphous polymer glass decreases with the decrease in isothermal compressibility and refractive index [6].

To consider optical properties of transparent optical organic materials, there is a need to prepare a very purified sample containing little contaminant to evaluate its optical transmission loss. Even a small amount of contaminants in the core polymer of a POF causes large attenuation loss because the optical path length of the POF is so long that the loss due to contaminant becomes integrated. Thus it is impossible to measure optical loss accurately. It is difficult with solid polymers to get a sufficiently purified sample, which has no contaminant [7].

Therefore, Takezawa, Taketani, Tanno and Ohara [8] have studied methods to estimate the optical loss of various polymers applicable for POFs as core material, especially for aromatic amorphous polymers, empirically from the chemical structure of a polymer-repeating unit. It is known that light scattering α_R is divided into two losses, that is, α^{iso} and α^{aniso}. Here, α^{iso} means the isotropic scattering loss; α^{aniso}, the anisotropic scattering loss. The α^{iso} is mainly a function of refractive index, and the α^{aniso} is a function of refractive index, density, and the number of benzene rings in the polymer repeating unit. Thus, when the polymer density and the structure of its repeating unit are known, the values of α_R can be estimated. They derived new empirical equations for predicting the values of each intrinsic light scattering loss, α^{iso} and α^{aniso} from several experiments.

3.1 Experimental

3.1.1 Materials

Tab. 3.1 lists the amorphous polymers used to measure intrinsic light scattering losses in this experiment. To eliminate the effect of unknown impurities, the purification method for Polycondensation type polymers, i.e., PC, polyarylate (PAr), polysulfone (PSF), and polyethersulfone (PES), were dissolved in dichloromethane and then filtered through a Teflon membrane filter (pore size: $0.2\,\mu m$). Addition polymerization type polymers, i.e., PMMA and polystyrene (PSt), were polymerized using their purified monomers. Their monomers were purified carefully by an ordinary procedure, rinsing the monomers with aqueous NaOH solution, and distilling them under reduced pressure [8].

Polymers	$M(g/mol)$	$\rho(g/cm^3)$
PMMA	100	1.19
PSt	104	1.07
PC	254	1.20
Par	358	1.21
PSF	442	1.22
PES	232	1.37

Table 3.1 Amorphous polymers [8].

3.1.2 Theory

To make and evaluate the experiment, Takezawa, Taketani, Tanno and Ohara [8] have used the theory, mentioned below, from Koike, Tanio and Ohtsuka [9].

When natural light with an intensity I_0 passes through a distance y and its intensity is decreased to I by the scattering loss, the turbidity τ is defined by Eq.(3.1). Since

$$I / I_0 = \exp(-\tau y) \tag{3.1}$$

the turbidity τ corresponds to the summation of all light scattered to all directions, τ is given by Eq.(3.2). Here symbols

$$\tau = \pi \int_0^{\pi} (V_V + V_H + H_V + H_H) \sin\theta \, d\theta \tag{3.2}$$

V and H denote vertical and horizontal polarizations, respectively. The symbol A of the scattering component A_B represents the direction of an analyzer and the subscript B

represents the direction of the polarizing phase of an incident light. θ is the scattering angle from the direction of the incident ray.

In structureless liquid or randomly oriented polymer bulk, these intensities are given by the following equations:

$$V_H = H_V \tag{3.3}$$

$$H_H = V_V \cos^2\theta + H_V \sin^2\theta \tag{3.4}$$

Almost all samples used in the experiment exhibited angular dependence in the V_V intensity due to large heterogeneities inside the bulk. Then, they separated V_V into two terms as written in Eq.(3.5), where V_{V1} denotes a background intensity

$$V_V = V_{V1} + V_{V2} \tag{3.5}$$

which is independent of the scattering angle and V_{V2} is the excess scattering with angular dependence due to large heterogeneities. The isotropic part V_{V1}^{iso} of the V_{V1} is given by Eq.(3.6). When there is no angular dependence in H_V, the

$$V_{V1}^{iso} = V_{V1} - 4/3\, H_V \tag{3.6}$$

angular dependence of V_V is attributed to the isotropic scattering V_{V2}^{iso}. Therefore

$$V_{V2} = V_{V2}^{iso} \tag{3.7}$$

By substitution of Eq.(3.3)-(3.7) into Eq.(3.2)

$$\tau = \pi \int_0^{\pi} \left\{ (1+\cos^2\theta)(V_{V1}^{iso} + V_{V2}^{iso}) + \frac{(13+\cos^2\theta)}{3} H_V \right\} \sin\theta \, d\theta \tag{3.8}$$

For the V_{V2}^{iso}. Debye et al. derived Eq.(3.9), where $<\eta^2>$ denotes the mean-square average of the fluctuation of all

$$V_{V2}^{iso} = \frac{4<\eta^2>\pi^3}{\lambda_0^4} \int_0^{\infty} \frac{\sin(\upsilon sr)}{\upsilon sr} r^2 \gamma(r) dr \tag{3.9}$$

dielectric constants, $\upsilon = 2\pi/\lambda$, and $s = 2\sin(\theta/2)$. λ and λ_0 are wavelengths of light in a specimen and under vacuum, respectively. $\gamma(r)$ refers to the correlation function defined by $\eta_i \eta_j / <\eta^2>$ where η_i, and η_j are the fluctuations of dielectric constants at; i and j positions. Assuming that the correlation function is expressed by Eq.(3.10) as suggested by Debye et al., Eq.(3.9) is simply integrated to give Eq.(3.11).

$$\gamma(r) = \exp(-r/a) \tag{3.10}$$

$$V_{V2}^{iso} = \frac{8\pi^3 <\eta^2> a^3}{\lambda_0^4 (1+\upsilon^2 s^2 a^2)^2} \qquad \upsilon = 2\pi n/\lambda_0, \quad s = 2\sin(\theta/2) \tag{3.11}$$

Here a is called the correlation length and is a measure of the size of the heterogeneous structure inside the bulk. The turbidity τ is divided into three terms. Namely

$$\tau = \tau_1^{iso} + \tau_2^{iso} + \tau^{aniso} \tag{3.12}$$

where τ_1^{iso} is the turbidity coming from the V_{V1}^{iso} scattering, τ_2^{iso} is from V_{V2}^{iso}, and τ^{aniso} is from the anisotropic scattering, H_V. From Eq.(3.8), these terms are given as follows:

$$\tau_1^{iso} = \int_0^{\pi} (1+\cos^2\theta) V_{V1}^{iso} \sin\theta \, d\theta = {}^{8}\!/_{3}\, \pi V_{V1}^{iso}, \tag{3.13}$$

$$\tau_2^{iso} = \frac{32a^3 < \eta^2 > \pi^4}{\lambda_0^4} \left\{ \frac{(b+2)^2}{b^2(b+1)} - \frac{2(b+2)}{b^3} \ln(b+1) \right\},$$

$$b = 4k^2 a^2 \tag{3.14}$$

$$\tau^{aniso} = {}^{80}\!/_{9}\, \pi H_V \tag{3.15}$$

The light-scattering loss α (dB/km) is related to the turbidity τ (cm^{-1}) by Eq.(3.16). The light scattering losses

$$\alpha \ (dB/km) = 4.342 \times 10^5 \ \tau \ (cm^{-1}) \tag{3.16}$$

corresponding to each turbidity of Eq.(3.12)-(3.15) are defined as α_t, α_1^{iso}, α_2^{iso} and α^{aniso}, respectively. That is

$$\alpha_t = \alpha_1^{iso} + \alpha_2^{iso} + \alpha^{aniso} \tag{3.17}$$

Again, these scattering losses in their treatment are based on the following two assumptions: (1) The H_V is independent of the scattering angle and no large anisotropic order exists. (2) The V_{V2}^{iso} given by Eq.(3.11) is superimposed on the constant background V_{V1}.

Polymerization temp, ^{0}C	a, ^{0}A	$<\eta^2>, 10^{-8}$	α_1^{iso} dB/km	α_2^{iso} dB/km	α^{aniso} dB/km	α_t dB/km
70	676	1.05	16.8	40.8	4.4	62.0
100	466	0.53	17.7	10.9	4.0	32.6
130		0	9.7	0	4.7	14.4

Table 3.2 Scattering Parameters of PMMA Glasses Polymerized at 70, 100, and 130^{0}C for 96h [9].

Before obtaining quantitative scattering data through the above analysis, they have to confirm the validity of the above two assumptions. For assumption 1, all PMMA samples prepared in their laboratory had no angular dependence in the H_V intensities, which were in the range $3-6\times10^{-7}\,cm^{-1}$, while many samples strongly exhibited the forward excess V_V scattering. Therefore, it is clear that the angular dependence was due to the isotropic heterogeneity and not due to the anisotropic order. Thus, assumption 1 seems reasonable in their experiment.

For assumption 2, it is difficult to experimentally discriminate the V_{V2}^{iso} component from the observed V_V. Thus the following procedure was carried out. By the rearrangement of Eq.(3.11), $V_{V2}^{-1/2}$ versus s^2 (Debye plot) gives a straight line, and the correlation length a can be determined by $a=(\lambda/2\pi)$ (slope/intercept)$^{1/2}$. Therefore by changing the V_{V2}^{iso} value between 0 and the observed V_V little by little, the V_{V2}^{iso} where the Debye plot became closest to a straight line was obtained by a least-square technique in a computer and was employed in data analysis.

With the increase in polymerization temperature, the total scattering loss α_t remarkably decreased from 62 to $14.4\,dB/km$, where α_2^{iso} from the isotropic V_{V2}^{iso} due to large

heterogeneities decreased from 41 dB/km to 0, although the anisotropic scattering loss α^{aniso} was almost invariant around 4-5 dB/km. It is clear from Table II that the excess V_V scattering expressing the angular dependence is not inherent in the PMMA bulk.

The intensity of the isotropic V_V^{iso} scattering from thermally induced density fluctuations in a structureless liquid is given by

$$V_V^{iso} = \frac{\pi^2}{9\lambda_0^4}(n^2-1)^2(n^2+2)^2 kT\beta \tag{3.18}$$

where k is the Boltzmann's constant, T the absolute temperature, and β the isothermal compressibility. With published values $\beta = 3.55\times10^{-11}\ cm^2/dyn$ around T_g for the PMMA bulk, assuming a frozen condition, the V_{V2}^{iso} calculated from Eq.(3.18) at room temperature for 633-nm wavelength is $2.61\times10^{-6}\ cm^{-1}$. By Eq.(3.13) and (3.16), the light-scattering loss from this V_{V2}^{iso} value is estimated to be 9.5 dB/km which is very close to 9.7 dB/km of the α_1^{iso} for the sample polymerized at 130 °C in Tab. 3.2. Therefore, if Eq.(3.18) using β at T_g is applicable to the polymer bulk, the value of 9.7 dB/km attained in Tab. 3.2 would be the limit of the isotropic scattering loss for the PMMA in the atmosphere.

3.1.3 Measurement of Light Scattering Loss

Fig. 3.1 gives a block diagram of the measurement apparatus for light scattering intensity. The light source was a He-Ne laser (wavelength, 633 nm), which was set up to obtain a vertical polarization. The laser beam was divided into two beams by a half mirror. One was directly monitored by a photomultiplier tube to compensate for fluctuation of the laser intensity. The other beam passed through a light chopper and

polarizer and then entered the rodlike sample from the side. The gap between the sample and the inner wall of the glass cell was filled with immersion oil (refractive index: 1.5). This glass cell was perpendicularly located on the center of the goniometer. The scattered light intensity (V_v, H_v) from the sample was detected by a photomultiplier [V_v (cm^{-1}): polarized scattering intensity]. From Eq.(3.19) the intensity V_v^{iso} of the isotropic scattering is obtained. The isotropic turbidity τ^{iso} (cm^{-1}) and the isotropic scattering loss α^{iso} (dB/m) due to V_v are estimated from Eq.(3.20), and the anisotropic turbidity τ^{aniso} (cm^{-1}) and the anisotropic scattering loss α^{iso} (dB/m) due to H_v are calculated from Eq.(3.21). The α_R is given by Eq.(3.22).

$$V_v^{iso} = V_v - \frac{4}{3} H_v \tag{3.19}$$

$$\alpha^{iso} = 4.342 \times 10^2 \times \tau^{iso} = 4.342 \times 10^2 \frac{8}{3} \pi V_v^{iso} \tag{3.20}$$

$$\alpha^{aniso} = 4.342 \times 10^2 \times \tau^{aniso} = 4.342 \times 10^2 \frac{80}{9} \pi H_V \tag{3.21}$$

$$\alpha_R = \alpha^{iso} + \alpha^{aniso} \tag{3.22}$$

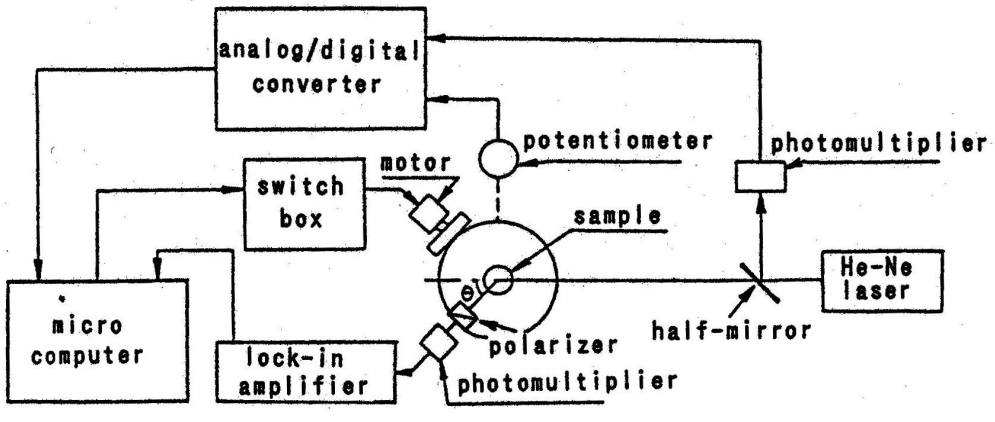

Figure 3.1 Diagram of light scattering measurement apparatus [8].

3.2 Results and Discussion

3.2.1 Prediction of Isotropic Scattering Loss

The α_R is divided into two losses as shown in Eq.(3.22). The isotropic scattering loss α^{iso} is further divided into two components, one is α_1^{iso}, which has no angular dependence, and the other is α_2^{iso}, which has an angular dependence due to heterogeneities existing in a polymer, i.e., fluctuation of density or refractive index of the polymer. α_2^{iso} can be decreased to a negligible magnitude by annealing, so that they used the approximation $\alpha_2^{iso} = 0$ in their study. They conformed that the measured α^{iso} curves of all polymers in Tab. 3.1 had no angular dependence. Thus they have defined α_R as the ultimate loss limit of a polymer, that is, intrinsic light scattering loss.

The intensity V_v^{iso} of the isotropic scattering from thermally induced density fluctuations in a structureless liquid is given by Eq.(3.23),

$$V_v^{iso} = \frac{\pi^2}{9\lambda^4}(n^2-1)^2(n^2+2)^2 kT\beta \tag{3.23}$$

where λ (cm) is the wavelength under vacuum, n is the refractive index, k $(=1.381\times10^{-16} erg/K)$ is the Boltzmann constant, T is the absolute temperature, and β (cm^2/dyn) is the isothermal compressibility at the glass transition temperature T_g. Thus α^{iso} (dB/m) is given by Eq.(3.24).

$$\begin{aligned}\alpha^{iso} &= 4.342\times10^2 \times \tau^{iso} \\ &= \frac{5.50\times10^{-13}}{\lambda^4}(n^2-1)^2\ (n^2+2\ )^2\ T\beta\end{aligned} \tag{3.24}$$

The α^{iso} is a function of the refractive index (n) and the isothermal compressibility (β) of its polymer. Then if both values were known, α^{iso} could be calculated accurately. However, Takezawa, Taketani, Tanno and Ohara could not easily obtain β values of all other polymers, so that it is difficult to calculate α^{iso} of all amorphous polymers from Eq.(3.24).

Tab. 3.3 lists values of n and β at the temperature over T_g of PMMA, PSt, PC, PAr, PSF, and PES. As shown in Tab. 3.3, values of β at the temperature over T_g for these polymers are the same order, from 5×10^{-11} to 8×10^{-11}. As for the other many amorphous polymers, their β values are within the extent. Thus they assumed that β and T_g was independent of the kind of polymers, that is, $\beta = 6.3\times10^{-11}\ cm^2/dyn$, and proposed the following equation to estimate $\alpha^{iso}\ (dB/m)$ empirically from the chemical structure of the polymer repeating unit:

$$\alpha^{iso} = \frac{1.0\times10^{-20}}{\lambda^4}(n^2-1)^2(n^2+2)^2 \tag{3.25}$$

Polymers	n	$(n^2-1)^2(n^2+2)^2$	$T_g\ (^0C)$	$\beta\ (cm^2/dyn)$
PES	1.65	66.2	230	-
PSF	1.63	59.5	189	$5.6\times10^{-11}(220^0C)$
Par	1.60	50.6	193	$7.0\times10^{-11}(250^0C)$
PC	1.59	47.9	150	$8.0\times10^{-11}(250^0C)$
PSt	1.59	47.9	100	$5.8\times10^{-11}(100^0C)$
PMMA	1.49	26.5	120	$5.2\times10^{-11}(120^0C)$

Table 3.3 Physical constants concerning α^{iso} [8].

3.2.2 Prediction of Anisotropic Scattering Loss

The intensity H_v of the anisotropic scattering is given by Eq.(3.26):

$$H_v = \frac{16\pi^2}{135\lambda^4}(n^2+2)^2 N\delta^2 \tag{3.26}$$

where $N\,(=N_0\times\rho/M)$ is the number of repeating unit in $1\,cm^3$ of a polymer, N_0 (=6.02×10^{23}) is the Avogadro number, $\rho\,(g/cm^3)$ is the density of a polymer, M (g/mol) is the molecular weight of repeating units, and δ^2 $(10^{-50}\,cm^6)$ is the mean square polarizability anisotropy of scattering centers. Therefore, α^{aniso} (dB/m) is given by Eq.(3.27).

$$\begin{aligned}\alpha^{aniso} &= 4.342\times10^2\times\tau^{aniso}\\ &= \frac{1.42\times10^4}{\lambda^4}(n^2+2\,)^2 N\delta^2\end{aligned} \tag{3.27}$$

It is a function of the refractive index (n), N, and δ^2. However, they could not easily obtain δ^2 values of all other polymers, so that it is difficult to calculate α^{aniso} of all amorphous polymers from Eq.(3.27). Therefore, if the value of δ^2 were known by an empirical procedure, they could estimate α^{aniso} from the chemical structure of its repeating unit of a polymer.

Tab. 3.4 shows values of n, N, and δ^2 of PMMA, PSt, and PC. Here, they assumed that δ^2 was a function of the number (p) of benzene rings in the polymer-repeating unit. As shown in Fig. 3.2, δ^2 was proportional to p^2, and $10^{-3}\times\delta^2 = 5p^2+0.3$.

Thus they derived the following equation to estimate $\alpha^{aniso}\ (dB/m)$ empirically from the chemical structure of the polymer-repeating unit:

$$\alpha^{aniso} = \frac{8.5\times10^{-19}}{\lambda^4}(n^2+2)^2\frac{\rho}{M}(5p^2+0.3) \tag{3.28}$$

Polymers	n	$(n^2+2)^2$	$N=\frac{\rho}{M}N_0$ (cm^{-3})	δ^2 $(10^{-50}cm^6)$	$(n^2+2)^2N\delta^2$
PC	1.59	20.5	2.8×10^{21}	21000	1.2×10^{-23}
PSt	1.59	20.5	6.2×10^{21}	5506	7.0×10^{-24}
PMMA	1.49	17.8	7.2×10^{21}	326	4.2×10^{-25}

Table 3.4 Physical constants concerning α^{aniso} [8].

3.2.3 Estimation of Light Scattering Loss by Empirical Equations

The values of α^{iso} and α^{aniso} estimated from Eq.(3.25) and Eq.(3.28) concerning PMMA, PSt, PC, PAr, PSF, and PES are shown in Tab. 3.5. The values estimated from Eq.(3.25) and Eq.(3.28) agreed well with the values that were calculated from Eq.(3.24) and Eq.(3.27) or observed with their samples. This indicates the validity of Eq.(3.25) and Eq.(3.28). They could not obtain reasonable values of α_R concerning PSF and PES because it was difficult to fabricate rodlike samples having no microvoids. Thus their values were very large, though their light scattering intensity had no angular dependence. Furthermore, the α_R of aromatic amorphous polymers was not so large inherently, and it was only a few hundred decibels per kilometer, at the highest.

Polymers	ρ / M (mol / cm^3)	n	p	$\alpha^{iso}(dB/m)$ Calculated Eq. (3.24)	$\alpha^{iso}(dB/m)$ Calculated Eq. (3.25)	$\alpha^{iso}(dB/m)$ Obs.	$\alpha^{aniso}(db/m)$ Calculated Eq. (3.27)	$\alpha^{aniso}(db/m)$ Calculated Eq. (3.28)	$\alpha^{aniso}(db/m)$ Obs.
PES	5.91×10^{-3}	1.65	2	-	0.041	-	-	0.142	-
PSF	2.76×10^{-3}	1.63	4	0.032	0.037	-	-	0.262	-
Par	3.38×10^{-3}	1.60	3	0.037	0.032	0.065	-	0.169	0.189
PC	4.72×10^{-3}	1.59	2	0.037	0.030	0.060	0.104	0.104	0.106
PSt	1.03×10^{-2}	1.59	1	0.028	0.030	0.021	0.060	0.059	0.060
PMMA	1.19×10^{-2}	1.49	0	0.014	0.017	0.012	0.002	0.003	0.005

Table 3.5 Estimation of light scattering losses of amorphous polymers (at λ=633 nm) [8].

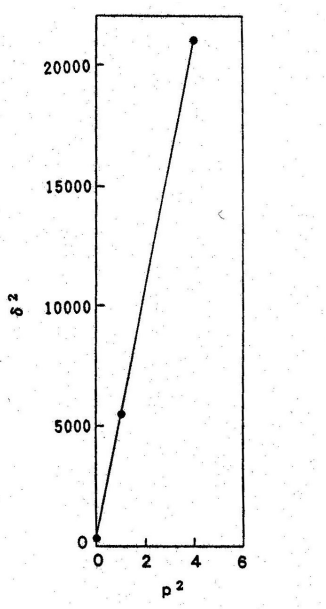

Figure 3.2 Relation between the square number (p^2) of benzene rings in the repeating unit of the polymer and the mean-square polarizability anisotropy of scattering centers (δ^2) [8].

3.2.4 Calculating Compressibility

As argued above, Rayleigh scattering is mainly caused by density fluctuations intrinsically present in (amorphous) polymers. Refractive index and compressibility are the two factors influencing the intensity of scattering. The compressibility (β) of an amorphous polymer is largely determined by its molecular volume or more specifically by the cross-sectional area, $A(\text{Å}^2)$, per polymer chain.

Using the fluctuation theory, the intensity of the isotropic light scattering (V_V^{iso}) from thermally induced density fluctuations in a structureless liquid is

$$V_v^{iso} = \frac{\pi^2}{9\lambda^4}(n^2-1)^2(n^2+2)^2 kT\beta \tag{3.29}$$

where λ_0 is the wavelength of light in vacuum, k is the Boltzmann constant, T is the absolute temperature, n is the refractive index, and β is the isothermal compressibility. The fluctuation theory for structureless liquids indicates that according to Eq.(3.29), the isotropic scattering loss decreases with the decrease in isothermal compressibility and refractive index. The value of V_V^{iso} calculated using the value of β at T_g according to a frozen model showed good agreement with the observed value for PMMA glass. When the reported β value at 100°C (near T_g) is used in Eq.(3.29), the calculated α^{iso} value is 9.5 dB/km which is close to our observed value (9.7 dB/km) for PMMA glass polymerized above the T_g in Fig. 3.3.

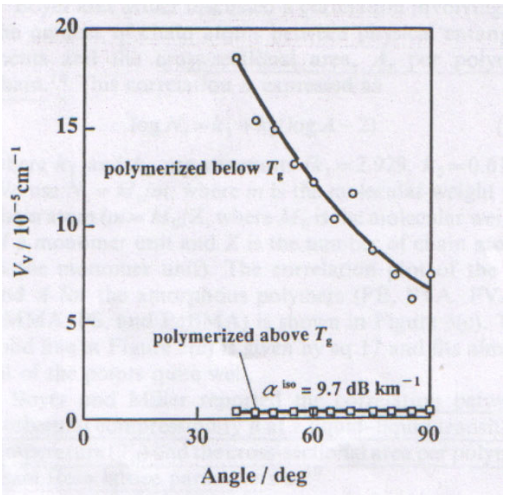

Figure 3.3 V_v scattering by PMMA glasses polymerized at 70^0C for 216h, and 130^0C for 96h [6].

In order to prepare low light-scattering-loss polymer glass, it is necessary to know the refractive index and the isothermal compressibility at T_g of polymers. However, the β for most polymers has not yet been measured precisely using a mechanical procedure. In order to estimate the β at T_g, Tanio and Koike [6] clarified following correlations between physical properties for amorphous polymers;

1. Relation between the intrinsic molecular volume (V_{int}) and actual molecular volume (V). (Correlation 1)

2. Relation between actual molecular volume (V) and molecular weight between chain entanglements (M_c). (Correlation 2)

3. Relation between the number of chain atoms between physical entanglements (N_c) and the cross- sectional area per polymer chain (A). (Correlation 3)

4. Relation between the cross-sectional area per polymer chain (A) and the isothermal compressibility at a liquid-liquid transition temperature (β at T_{11}). (Correlation 4)

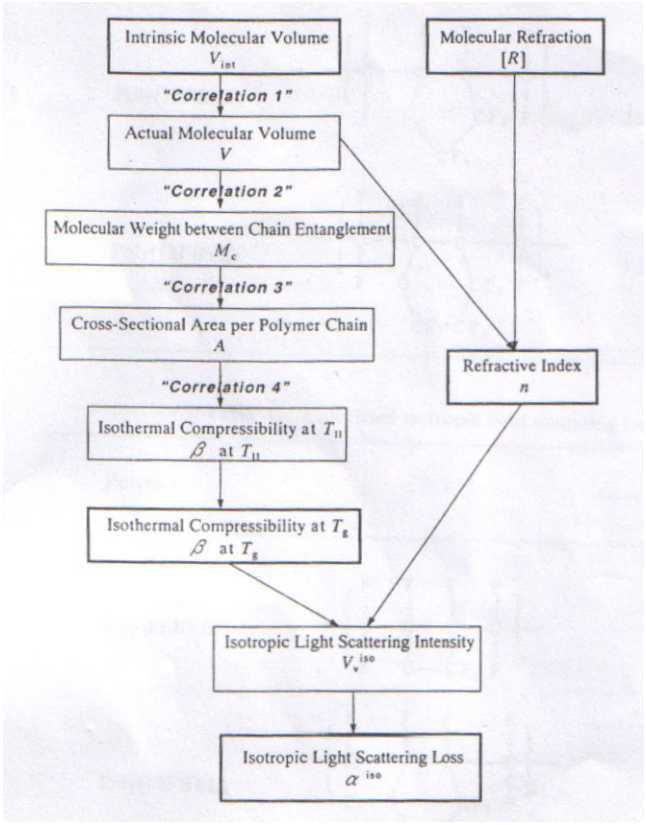

Figure 3.4 Method of estimating light scattering loss of amorphous polymer glass from its molecular structure [6].

The intrinsic molecular volume V_{int} of monomer unit for amorphous polymer can be calculated from the atomic radius and bond length of the constituent atoms based on the method developed by Slonimskii *et al.* When an atom B (atomic radius *R)* is bound to atom B_i (atomic radius R_i with bond length d_i, the atomic volume $\Delta V(B)$ of atom B is given by

$$\Delta V(B) = (4/3)\pi R^3 - \sum_i (1/3)\pi h_i^2 (3R - h_i)$$

$$h_i \equiv R - (R^2 + d_i^2 - R_i^2)/(2d_i) \qquad (3.30)$$

If the molecule consists of atoms $B_1 - B_j$ the intrinsic molecular volume V_{int} is given by

$$V_{\text{int}} = N_A \sum_j \Delta V(B_j) \tag{3.31}$$

where N_A is Avogadro's number. The actual molecular volume (V) of the monomer unit is obtained from the value of density (ρ) of polymer using

$$V = \frac{M_0}{\rho} \tag{3.32}$$

The actual molecular volume V is expressed as

$$V = \frac{V_{\text{int}}}{K} \tag{3.33}$$

where K is the packing coefficient of the molecule. Fig. 3.5a shows the $V - V_{\text{int}}$ plot for amorphous polymers (polyethylene(PE), polyvinyl alcohol(PVA), poly(vinyl acetate) (PVAc), PMMA, PS, and poly(*n*-butyl methacrylate) (P*n*BMA)). From Fig. 3.5a, it has been seen that the K value for typical amorphous polymers is about 0.68. Thus, the actual molecular volume can be estimated from V_{int} using $K = 0.68$.

Hoffmann found a linear correlation between the molecular weight between chain entanglements (M_c) and the square of the actual molecular volume of the monomer unit. He obtained the correlation $M_c \propto V^2$. On the other hand, Boyer and Miller suggested the correlation $M_c \propto V^{1.67}$. In order to confirm the correlation between M_c and V for amorphous polymers, Tanio and Koike [6] collected data on the M_c of the amorphous polymers (PE, PVA, PVAc, PMMA, PS, and P*n*BMA*).* Fig. 3.5b shows the $M_c - V^{1.67}$ plot for the amorphous polymers.

$$M_c = 18.3V^{1.67} \tag{3.34}$$

The solid line in Fig. 3.5b is given by Eq.(3.34). Boyer's relation had a better linearity than Hoffmann's relation for the amorphous polymers in Fig. 3.5b.

Boyer and Miller [13] discussed a correlation involving N_c the number of chain atoms between physical entanglements and the cross-sectional area, A, per polymer chain. This correlation is expressed as

$$\log N_c = k_1 + k_2(\log A - 2) \tag{3.35}$$

where k_1 and k_2 are constants ($k_1 = 2.929$, $k_2 = 0.614$). They use N_c=M_c/m, where m is the molecular weight per chain atom *(*m = M_0/Z, where M_0 is the molecular weight of a monomer unit and Z is the number of chain atoms in the monomer unit). The correlation plot of the N_c and A for the amorphous polymers (PE, PV A, PV Ac, PMMA, PS, and P*n*BMA) is shown in Fig. 3.5c. The solid line in Fig. 3.5c is given by Eq.(3.35) and fits almost all of the points quite well.

Boyer and Miller [14] reported the correlation between isothermal compressibility β at a liquid-liquid transition temperature (T_{ll}) and the cross-sectional area per polymer chain from lattice parameters as

$$\log(10^{11}\beta_{at\ T_{ll}}) = -0.21 + 0.55\log A \tag{3.36}$$

The liquid-liquid transition temperature appears to be a useful liquid-state reference temperature and is usually found by a variety of dynamic, thermodynamic methods. The concept of a T_{ll} was vigorously studied by Boyer. He found that T_{ll} is near $1.2T_g$ for

most polymers. Lobanov and Frenkel [15] have estimated T_{ll} for a variety of polymers from dielectric loss data and proposed an empirical relation between T_g and T_{ll}.

$$T_{ll} = T_g + 76(K) \tag{3.37}$$

For T_{ll} from $250K$ to $500K$, the numerical difference between the two empirical rules is slight.

In order to confirm the validity of Eq.(3.36) for amorphous polymers, Tanio and Koike [6] collected data on the cross-sectional areas and isothermal compressibilities of the amorphous polymers. Fig. 3.5d shows the log-log correlation of isothermal compressibility β at T_{ll} with the cross-sectional area per polymer chain in Å^2 for the amorphous polymers (polyisoprene (PI), polypropylene (PP), polyisobutylene (PIB), PVAc, PMMA, PS, P*n*BMA and poly(cyclohexyl methacrylate) (PCHMA)). The solid line in Fig. 3.5d is given by Eq.(3.36).

By combining the above relationship, the isothermal compressibility β at T_{ll} can be calculated from the intrinsic molecular volume V_{int}. But we should know the value of isothermal compressibility at T_g of polymers in order to estimate light scattering loss in glassy state. The isothermal compressibility β of polymers increases linearly with T from T_g to T_{ll}. Thus we should know the slope $d\beta / dT$ in the range between T_g and T_{ll} in order to estimate isothermal compressibility at T_g. It is interesting that the values of $(1/\beta_{at\ T_{ll}})(d\beta / dT)$ in the range between T_g and T_{ll} for several amorphous polymers are almost the same (average value is $4.8\times10^{-3}K^{-1}$). When we use this value ($(1/\beta_{at\ T_{ll}})(d\beta / dT) = 4.8\times10^{-3}K^{-1}$ at $T_g < T < T_{ll}$) and the empirical relationship between T_{ll} and T_g ($T_{ll} = T_g 76(K)$), we can estimate the isothermal compressibility at T_g from the value of β at T_{ll}.

Tab. 3.6 shows the isothermal compressibilities of amorphous polymers (PMMA and PS) estimated from their molecular volume. These calculated values are in good agreement with observed values obtained from dilatometric method.

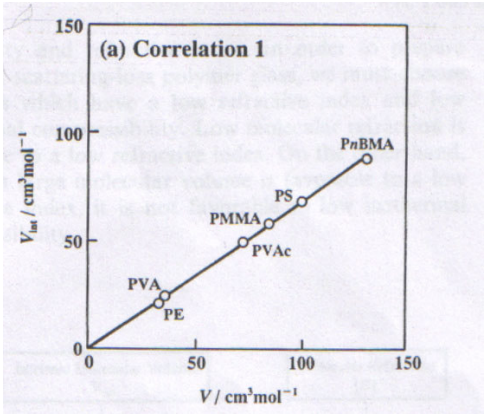

Figure 3.5(a) Correlations between physical properties for amorphous polymers; relation between V_{int} and V_{ll} [6].

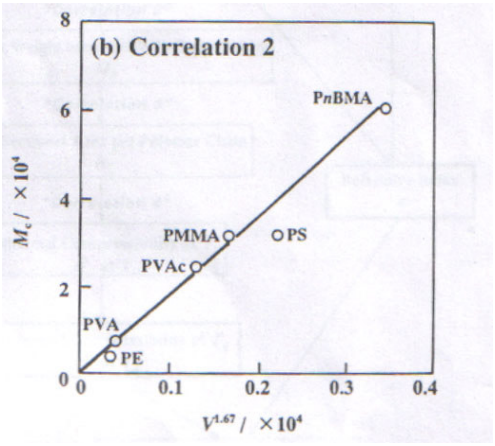

Figure 3.5(b) Correlations between physical properties for amorphous polymers; relation between V and M_c [6].

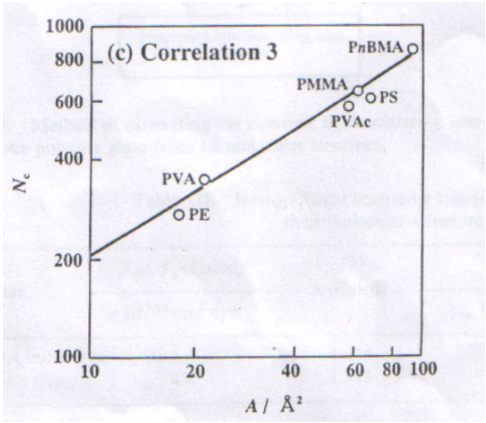

Figure 3.5(c) Correlations between physical properties for amorphous polymers; relation between N_c and A [6].

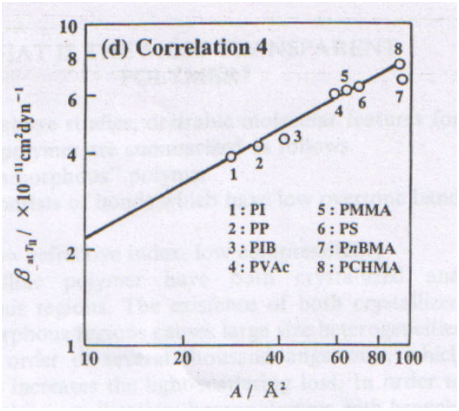

Figure 3.5 (d) Correlations between physical properties for amorphous polymers. relation between A and $\beta_{at\ Tll}$ [6].

Polymer	V_{int} (Cal)	V (Cal)	M_c (Cal)	A (Cal)	β at T_{ll} /$\times 10^{-11}$		β at T_g /$\times 10^{-11}$	
	cm^3mol^{-1}	cm^3mol^{-1}	$\times 10^4$	$^0A^2$	Cal	Obsd	Cal	Obsd
PMMA	57.7	84.9	3.05	58.3	5.8	6.1	3.6	3.6
PS	67.6	99.4	3.96	82.4	7.0	7.3	4.4	5.0

Table 3.6 Isothermal compressibilities *(β)* of amorphous polymers calculated from their molecular structure in comparison with observed values [6].

3.3 Some Important Points on Empirical Prediction Method of Intrinsic Light Scattering Loss of Transparent Amorphous Polymers

Consequently, if the polymer density and the structure of its repeating unit are known, the intrinsic light scattering losses can be estimated by using those equations without any experimental measurements.

CHAPTER 4

NUMERICAL SOLUTIONS ON LIGHT SCATTERING LOSS IN PLASTIC OPTICAL FIBERS

In the last few years, interest in polymer optical fibers (POF) has increased because of their low cost, easy handling and good flexibility even at large diameters. Moreover, optical cables do not have the problem of electromagnetic interference, which gives, for instance, the problem of cross-talk in copper telephone cables. In the usage of current communication and computer systems the yield has gained a big importance and it has seen from studies that light scattering loss is the only loss, which cannot be eliminated entirely. Besides, this loss causes its attenuation loss intrinsically and determines the lower limit of loss in the POF.

Rayleigh scattering occurs as a result of small density fluctuations, produced during the fabrication process. When an optical fiber is formed, the glass is pulled through an oven, where the molten material is stretched to become a thin fiber. After leaving the oven it freezes back into an amorphous solid. There is a high level of thermal agitation at the transition temperature (melting point) of glass, and this thermodynamical disorder leads to compositional and density fluctuations. These random variances are frozen in, and serve as the source for subsequent Rayleigh scattering. This is a fundamental process: there is nothing that can be done to eliminate the thermal agitation that accompanies melting thermal material for manufacture of waveguides.

While studying this thesis, a computer program was written to calculate light scattering loss in plastic optical fibers for different polymers. This program was written with using PHP language, and the codes are given in (App.A)[1].

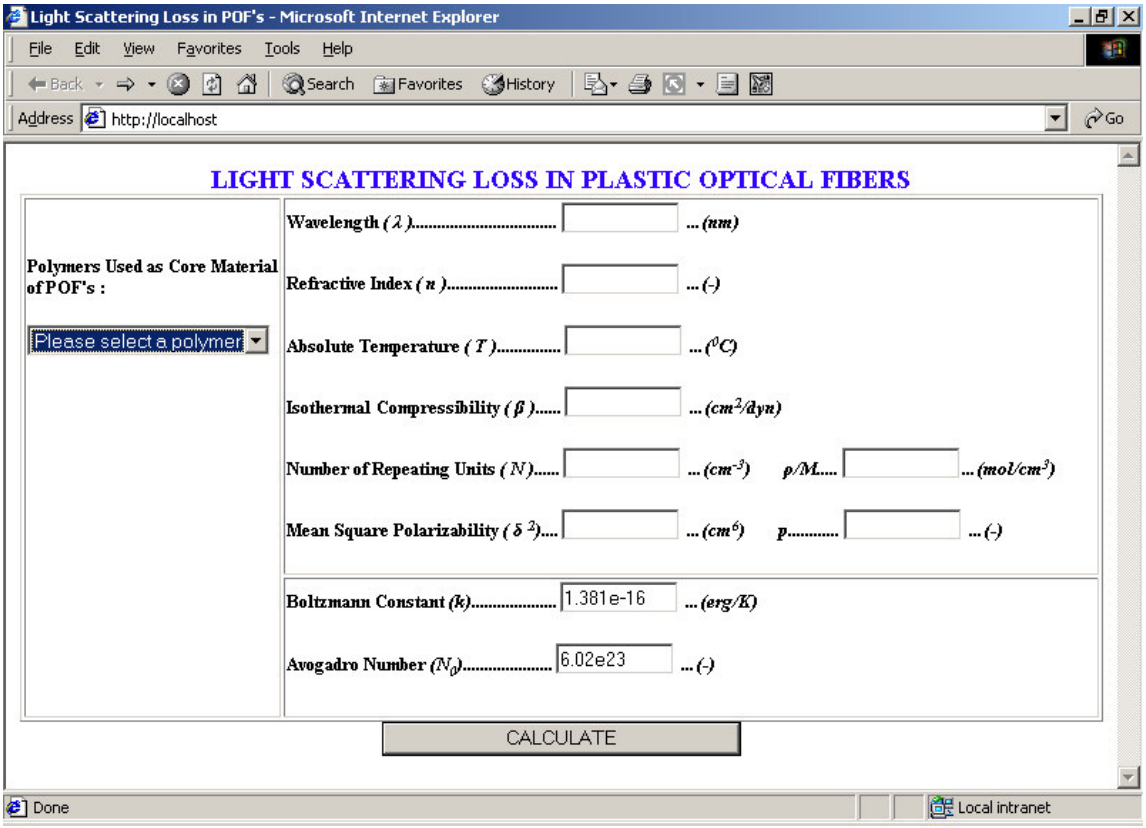

Figure 4.1 The selection screen of the program.

In this program, light scattering of six different polymers -PMMA, PSt, PC, PAr, PSF, PES- can be calculated. After selecting the polymer from left hand side, this polymer's data, which is taken from Tab. 3.3 and Tab. 3.4 as reference, is shown at right hand side. Also the program gives user the permission of changing each data. Afterwards, theoretical and empirical values of α_{iso}^{1}, α_{aniso} and α_{t} of selected polymer can be calculated by pressing "CALCULATE" button. Here α_{iso}^{1} is angular independent part of

[1] It can be also reached from the site: http:\\burak.sayel.com.tr

the isotropic scattering loss, α_{aniso} is the anisotropic scattering loss, and α_t is the total scattering loss.

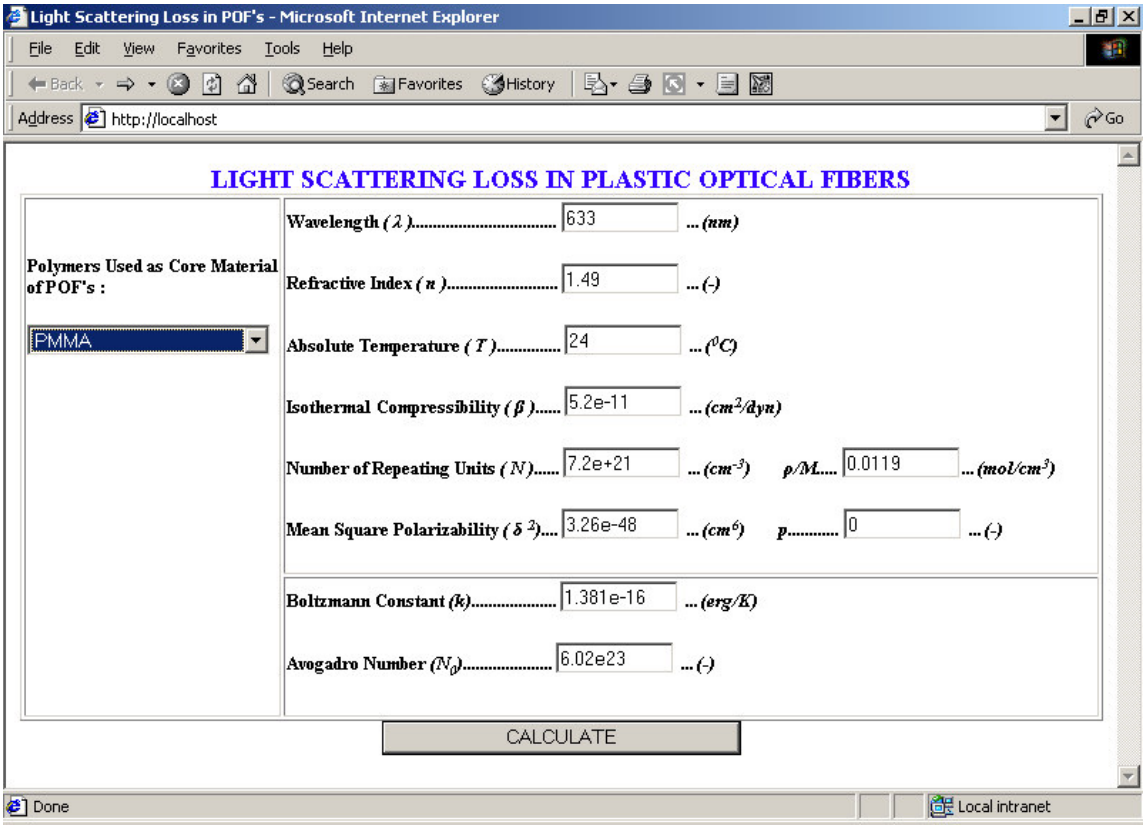

Figure 4.2 Data screen used in calculation of PMMA.

In Fig. 4.2 the data screen of PMMA can be seen. Data and result screens of other polymers are given in (App.B). Light scattering loss depends on; wavelength of light source (λ), absolute temperature of the medium (T), and refractive index (n), isothermal compressibility (β), number of repeating units (N), mean square polarizability anisotropy of scattering centers (δ^2), ρ / M (mol / cm^3), number of benzene rings in the polymer repeating unit (p) of the polymer. Therefore, all these parameters are used during the calculation process, and light scattering loss alters, when any of these parameters is changed.

The results that are obtained from using the data in Fig. 4.2 are shown in Fig. 4.3. At the result screen, the user can evaluate if the empirical equations, suggested before, provide the theoretical ones. Also, it can be seen that there is small difference between theoretical and empirical results in Fig. 4.3.

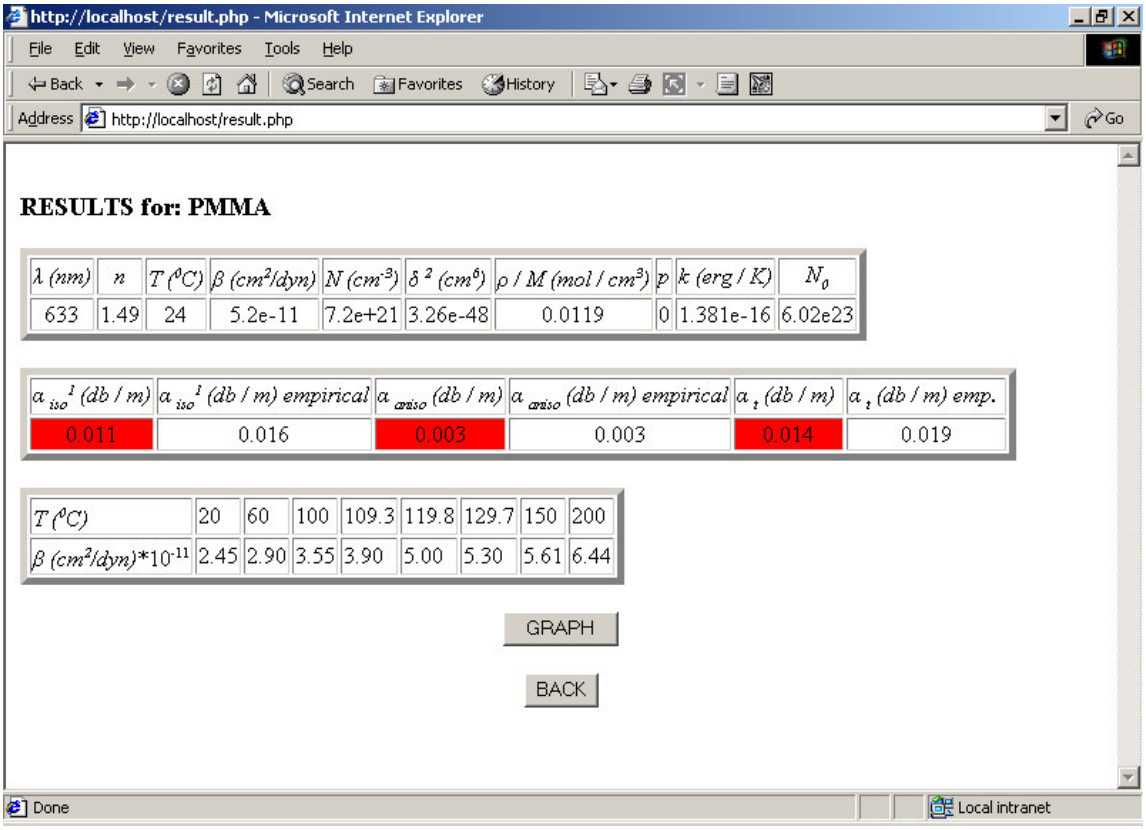

Figure 4.3 The outputs of results after the calculation for PMMA.

Temperature $T(^0C)$	20	60	100	109.3	119.8	129.7	150	200
Iso. comp. $\beta(cm^2/dyn)\times10^{-11}$	2.45	2.90	3.55	3.90	5.00	5.30	5.61	6.44

Table 4.1 The values of isothermal compressibilities of PMMA at different temperatures [12].

In addition, the graph of isotropic scattering loss versus isothermal compressibility can be plotted for various polymers. In this study, this graph is applied for only one sample, called PMMA. In the program, by using “GRAPH” button in Fig. 4.3 isotropic scattering loss versus isothermal compressibility graph can be plotted for PMMA. The graph is also shown in Fig. 4.4.

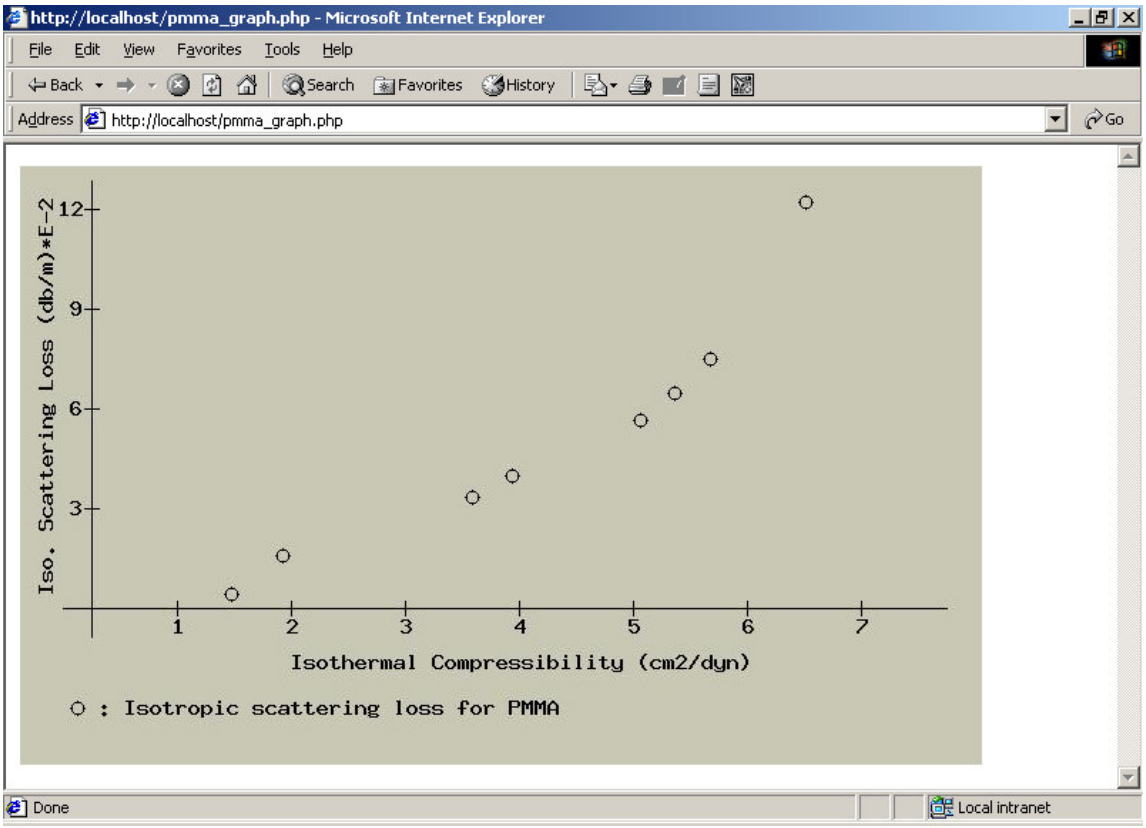

Figure 4.4 The graph of isotropic scattering loss versus isothermal compressibility.

The graph of isotropic scattering loss versus isothermal compressibility shows that isotropic scattering loss increases rapidly while the isothermal compressibility increases. We can see the ratio between isothermal compressibility and isotropic scattering loss clearly that proofs the expectation from Eq.(3.24).

In addition, if the “calculate all” choice is selected from polymers combo box in Fig. 4.1, the graph of total attenuation loss versus wavelength will be plotted as shown in Fig. 4.5.

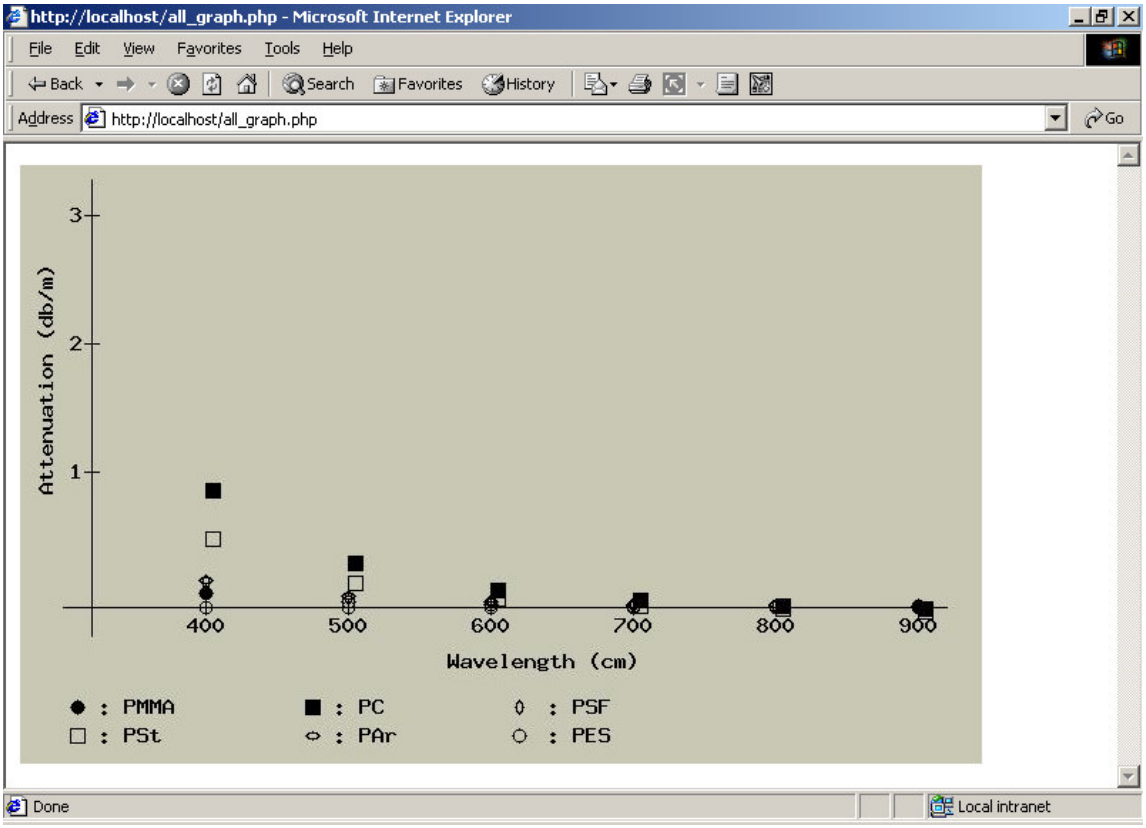

Figure 4.5 The graph of total attenuation loss versus wavelength.

The behavior of total attenuation loss for various wavelengths can be seen in Fig. 4.5. As expected, total attenuation loss decreases when wavelength increases. It is known that total attenuation loss is inversely proportional with the fourth power of wavelength. It can be seen from the graph that, PC has the largest value of attenuation in small wavelengths and PES has the smallest. However, we do not have all necessary data to calculate total attenuation loss for PES. Therefore, PES must not be taken into consideration. In this manner, PMMA has the smallest attenuation loss. As a result, it can be said that PMMA is more appropriate polymer for using as core material of POFs. In fact, PMMA is preferred as a core material for POFs in current communication and

computer systems. Furthermore, total attenuation losses for all polymers decrease and become closer, while wavelength increases. In this study, wavelength is taken 633 nm which is in the visible region. These polymers have good transparency in the visible region and have optical windows, that is, a low loss region, near 660 nm.

CHAPTER 5

CONCLUSIONS

In this work, the importance and the dependencies of light scattering were studied, and calculations were done in order to find more appropriate polymer for using as core material of POFs. For this aim, a computer program that calculates the light scattering loss of several amorphous polymers and plots the graph of isotropic scattering loss versus isothermal compressibility and total attenuation loss versus wavelength was written.

It is understood from the Takezawa, Taketani, Tanno and Ohara's study [8] that it is difficult with solid polymers to get a sufficiently purified sample, which has no contaminant to consider optical properties of transparent optical organic materials. There is a need to prepare a very purified sample containing little contaminant to evaluate its optical transmission loss. Even a small amount of contaminants in the core polymer of a POF causes large attenuation loss because the optical path length of the POF is so long that the loss due to contaminant becomes integrated. Thus it is impossible to measure optical loss accurately. Therefore, they suggested some empirical assumptions. Then we examined these assumptions by applying the program mentioned above.

Applying the data given in Takezawa, Taketani, Tanno and Ohara's studies [7], [8] to our program, we can analyze if the empirical equations coincide with the theoretical ones.

From the graphs plotted by our program, it can easily be seen that, as expected, the isotropic light scattering loss of amorphous polymer glass increases rapidly while the isothermal compressibility increases. Moreover, total attenuation loss decreases when wavelength increases. Also, it is known that total attenuation loss is inversely proportional with the fourth power of wavelength. In addition, total attenuation losses for all polymers decrease and become closer, while wavelength increases.

After the calculations, the total light scattering loss of PMMA was found approximately 16 dB/km, which is not a large value of attenuation loss for a plastic optical fiber. Therefore, we can say that PMMA is the most proper amorphous polymer used as core material of POFs among the analyzed other five polymers.

Consequently, if the polymer density and the structure of its repeating unit are known, we can estimate the intrinsic light scattering losses using those equations without any experimental measurements.

REFERENCES

[1] http://www.ub.rug.nl/eldoc/dis/science/t.a.c.flipsen/c1.pdf

[2] http://students.washington.edu/hreeve/

[3] http://matlb.kjist.ac.kr/~optoelec/research/pof/pof.html

[4] C.R. Pollock, *Fundamentals of Optoelectronics*. Chicago: Irwin, 1995 pp. 180-183.

[5] J.D. Jackson, *Classical Electrodynamics*. New York: Wiley, 1998 pp. 456-471.

[6] N. Tanio and Y. Koike, "What is the most transparent polymer?", *Polymer Journal*, Vol. 32, No. 1, pp. 43-50, 2000.

[7] Y. Takezawa, N. Taketani, S. Tanno, and S. Ohara, "Empirical estimation method of intrinsic loss spectra in transparent amorphous polymers for plastic optical fibers," *Journal of Applied Polymer Science*, Vol. 46, pp. 1835-1841, 1992.

[8] Y. Takezawa, N. Taketani, S. Tanno, and S. Ohara, "Empirical prediction method of intrinsic light scattering loss of transparent amorphous polymers," *Journal of Applied Polymer Science*, Vol. 46, pp. 2033-2037, 1992.

[9] Y. Koike, N. Tanio, and Y. Ohtsuka, "Light scattering and heterogeneities in low-loss poly(methyl methacrylate) glasses," *Macromolecules*, 22, pp. 1367-1373, 1989.

[10] http://211.132.9.28/pofeskae/tece/whatspofe/whatspof3e/whatspof3e.htm

[11] http://211.132.9.28/pofeskae/tece/whatspofe/whatspof4e/whatspof4e.htm

[12] J. Brandrup and E.H. Immergut, *Polymer Handbook*. New York: Wiley, 1989 pp. v/77-v/79.

[13] R. F. Boyer and R. L. Miller, *Rubber Chem. Technol.,* 51, 718, 1978.

[14] R. F. Boyer and R. L. Miller, *Macromolecules,* 17, 365, 1984.

[15] A. M. Lobanov and S. Ya. Frenkel, *Polym. Sci. USSR,* 22, 1150, 1980.

APPENDIX-A

Code of the Selection Screen

```
<html>

<head>
<title>Light Scattering Loss in POF's</title>


<SCRIPT LANGUAGE="JavaScript1.2">
function view(secme)
	{
	var endeks, selectedPolymer

	endeks=secme.selectedIndex
	selectedPolymer=secme.options[endeks].text

	if (selectedPolymer == "PMMA")
		{
		document.polymerForm.lambda.value=633
		document.polymerForm.index.value=1.49
		document.polymerForm.temp.value=24
		document.polymerForm.beta.value=5.2e-11
		document.polymerForm.N.value=7.2e21
		document.polymerForm.deltasq.value=326e-50
			document.polymerForm.rho.value=1.19e-2
		document.polymerForm.p.value=0
			document.polymerForm.all.value=0
			document.polymerForm.all.value="PMMA"
		}
	if (selectedPolymer == "PC")
		{
		document.polymerForm.lambda.value=633
		document.polymerForm.index.value=1.59
```

```
        document.polymerForm.temp.value=24
        document.polymerForm.beta.value=8.0e-11
        document.polymerForm.N.value=2.8e21
        document.polymerForm.deltasq.value=21000e-50
                document.polymerForm.rho.value=4.72e-3
        document.polymerForm.p.value=2
                document.polymerForm.all.value=0

        }

if (selectedPolymer == "PSt")
        {
        document.polymerForm.lambda.value=633
        document.polymerForm.index.value=1.59
        document.polymerForm.temp.value=24
        document.polymerForm.beta.value=5.8e-11
        document.polymerForm.N.value=6.2e21
        document.polymerForm.deltasq.value=5506e-50
                document.polymerForm.rho.value=1.03e-2
        document.polymerForm.p.value=1
                document.polymerForm.all.value=0

        }
   if (selectedPolymer == "PAr")
        {
        document.polymerForm.lambda.value=633
        document.polymerForm.index.value=1.6
        document.polymerForm.temp.value=24
        document.polymerForm.beta.value=7.0e-11
        document.polymerForm.N.value="-"
        document.polymerForm.deltasq.value="-"
                document.polymerForm.rho.value=3.38e-3
        document.polymerForm.p.value=3
                document.polymerForm.all.value=0

        }
   if (selectedPolymer == "PSF")
        {
        document.polymerForm.lambda.value=633
        document.polymerForm.index.value=1.63
        document.polymerForm.temp.value=24
        document.polymerForm.beta.value=5.6e-11
        document.polymerForm.N.value="-"
        document.polymerForm.deltasq.value="-"
                document.polymerForm.rho.value=2.76e-3
```

```
                document.polymerForm.p.value=4
                        document.polymerForm.all.value=0

                }
          if (selectedPolymer == "PES")
                {
                document.polymerForm.lambda.value=633
                document.polymerForm.index.value=1.65
                document.polymerForm.temp.value=24
                document.polymerForm.beta.value="-"
                document.polymerForm.N.value="-"
                document.polymerForm.deltasq.value="-"
                        document.polymerForm.rho.value=5.91e-3
                document.polymerForm.p.value=2
                        document.polymerForm.all.value=0}
         if (selectedPolymer == "Please select a polymer")
                {
                document.polymerForm.lambda.value=""
                document.polymerForm.index.value=""
                document.polymerForm.temp.value=""
                document.polymerForm.beta.value=""
                document.polymerForm.N.value=""
                document.polymerForm.deltasq.value=""
                        document.polymerForm.rho.value=""
                document.polymerForm.p.value=""
                        document.polymerForm.all.value=0

                }
          if (selectedPolymer == "Calculate All")
                {
                document.polymerForm.lambda.value=" "
                document.polymerForm.index.value=""
                document.polymerForm.temp.value=""
                document.polymerForm.beta.value=""
                document.polymerForm.N.value=""
                document.polymerForm.deltasq.value=""
                        document.polymerForm.rho.value=""
                        document.polymerForm.p.value=""
                        document.polymerForm.all.value=1
                }

        }
</SCRIPT>

      <script language="Javascript">
```

```
          function control() {
          if (document.polymerForm.lambda.value == "")
                        {alert("Please select a polymer or insert required values");
            document.polymerForm.polymerlist.focus();
            return false;}

        return true;}
         </script>

</head>

<body>

<CENTER><font color="#3300ff" size="4"><b>LIGHT SCATTERING LOSS IN
PLASTIC OPTICAL FIBERS</b></font></CENTER>

<table border="1" width="100%" height="370">
  <tr>
    <td width="24%" rowspan="6" height="364" valign="top"> 
      <p><b><font size="2">Polymers Used as Core Material of POF's :</font></b></p>
      <form NAME="polymerForm"  action="result.php" method="post"
onSubmit="return control();">

<input type="hidden" name="all">

        <p><select NAME="polymerlist" onChange="view(this)">
          <OPTION SELECTED>Please select a polymer
          <option >PMMA
          <option >PSt
                        <option >PC
                        <option >PAr
                        <option >PSF
                        <option >PES
                        <option >Calculate All
        </select></p>
            </td>
    <th width="76%" height="261" valign="top" nowrap>


        <p align="left"><b><font size="2">Wavelength <i>( &#955
        )..... </i></font></b><input name="lambda" VALUE=""
size="10" >
        <font size="2">... <i>(nm)</i></font>
        </p>
        <p align="left"><b><font size="2">Refractive Index <i>( n )</i>.....
```

```
      </font></b><input  name="index" size="10"> <font size="2">... <i>(-
)</i></font></p>

      <p align="left"><font size="2">Absolute Temperature <i>( T )</i>.....
      </font><input  name="temp" size="10"> <font size="2">...
<i>(<sup>0</sup>C)</i></font></p>
      <p align="left"><font size="2">Isothermal</font>
      <font size="2"> Compressibility <i>( &#946 )</i>..... </font><input  name="beta"
size="10">
      <font size="2">... <i>(cm<sup>2</sup>/dyn)</i></font></p>
      <p align="left"><font size="2">Number of Repeating Units <i>( N )</i>.....
      </font><input  name="N" size="10"> <font size="2">... <i>(cm<sup>-
3</sup>)       
      &#961/M..... </i></font><input  name="rho" size="10"><font size="2">...
<i>(mol/cm<sup>3</sup>)</i></font></p>
    <p align="left"><font size="2">Mean Square Polarizability <i>( &#948
<sup>2</sup>)</i>....
    </font><input  name="deltasq" size="10"> <font size="2">...
<i>(cm<sup>6</sup>)       
    p..... </i></font><input  name="p" size="10"> <font size="2">... <i>(-
)</i></font>
    </p>
   </th>
  </tr>
  <tr>
   <td width="76%" height="97" valign="top">
    <p style="line-height: 100%"><b><font size="2">Boltzmann Constant
<i>(k)</i>.....
    </font></b><input  name="T1" size="10" value="1.381e-16"> <font
size="2"><b>...
    <i>(erg/K)</i></b></font><p style="line-height: 100%"><font
size="2"><b>Avogadro
    Number </b> <i><b>(N<sub>0</sub>)</b></i><b>.....
</b></font><input  name="T1" size="10" value="6.02e23">
    <font size="2"><b>... </b>
    <i><b>(-)</b></i></font></td>
  </tr>
</table>

<CENTER><input type="submit" name="submit" OnClick="Control()"       value="
CALCULATE              "></CENTER>
</form>
</body>

</html>
```

Code of the Result Screen

```
<?php
define ("PI","3.14159265");
define ("BOLTZMANN","1.381e-16");  //erg/K
define ("AVOGADRO","6.02e23");
$B=BOLTZMANN;
$A=AVOGADRO;

$lambda=$HTTP_POST_VARS['lambda'];
$index=$HTTP_POST_VARS['index'];
$temp=$t=$HTTP_POST_VARS['temp'];
$beta=$HTTP_POST_VARS['beta'];
$N=$HTTP_POST_VARS['N'];
$deltasq=$HTTP_POST_VARS['deltasq'];
$P=$HTTP_POST_VARS['p'];
$rho=$HTTP_POST_VARS['rho'];
$polymer=$HTTP_POST_VARS['polymerlist'];
$all=$HTTP_POST_VARS['all'];


        //changing units (nm->cm)
$lambda=$lambda*1e-7;

        //powers of lambda & ref. index
$lambda4=$lambda*$lambda*$lambda*$lambda;
//print("<big><b>...lambda4=</b></big>$lambda4\n");
$index2=$index*$index;

?>

<?php
        //calc. for all (start)

if ($all == 1)
{
$dizi1 = array ("PMMA","PSt","PC","PAr","PSF","PES");
$dizi2 = array(
        array("l"=>633e-7,"n"=>1.49,"t"=>24,"b"=>5.2e-11,"N"=>7.2e21,"d"=>3.26e-
48,"ro"=>1.19e-2,"p"=>0),
                array("l"=>633e-7,"n"=>1.59,"t"=>24,"b"=>5.8e-
11,"N"=>6.2e21,"d"=>5.506e-47,"ro"=>1.03e-2,"p"=>1),

array("l"=>633e-7,"n"=>1.59,"t"=>24,"b"=>8e-11,"N"=>2.8e21,"d"=>2.1e-
46,"ro"=>4.72e-3,"p"=>2),
```

```
                    array("l"=>633e-7,"n"=>1.6,"t"=>24,"b"=>7e-
11,"N"=>0,"d"=>0,"ro"=>3.38e-3,"p"=>3),

array("l"=>633e-7,"n"=>1.63,"t"=>24,"b"=>5.6e-11,"N"=>0,"d"=>0,"ro"=>2.76e-
3,"p"=>4),
                    array("l"=>633e-
7,"n"=>1.65,"t"=>24,"b"=>0,"N"=>0,"d"=>0,"ro"=>5.91e-3,"p"=>2),
                    );

          $fp=fopen("variable_all.php","w");
for ($i = 0 ; $i <= 5; $i++)
  {
   // print $i;
   //echo $dizi1[$i];

            $dizi2[$i]["l"]=400*1e-7;

            for ($k = 0; $k <=5; $k++)
              {
$totalpha=0;
$alphaiso1=0;
$alphaaniso=0;
$Vv1=0;
$Hv=0;
                    //calc. of isotropic scattering loss 1
$Vv1=(PI*PI* ($dizi2[$i]["n"]*$dizi2[$i]["n"]-1)*($dizi2[$i]["n"]*$dizi2[$i]["n"]-1)*
($dizi2[$i]["n"]*$dizi2[$i]["n"]+2)*
($dizi2[$i]["n"]*$dizi2[$i]["n"]+2)*
BOLTZMANN*$dizi2[$i]["t"]*$dizi2[$i]["b"])
/(9*$dizi2[$i]["l"]*$dizi2[$i]["l"]*$dizi2[$i]["l"]*$dizi2[$i]["l"]
);
$alphaiso1=4.342e3*(8/3)*PI*$Vv1;    //(db/m)
$alphaiso1=substr($alphaiso1,0,5);

            //calc. of anisotropic scattering loss
$Hv=(16*PI*PI*
($dizi2[$i]["n"]*$dizi2[$i]["n"]+2)*
($dizi2[$i]["n"]*$dizi2[$i]["n"]+2)*
$dizi2[$i]["N"]*$dizi2[$i]["d"])/
(135*$dizi2[$i]["l"]*$dizi2[$i]["l"]*$dizi2[$i]["l"]*$dizi2[$i]["l"]);
$alphaaniso=4.342e3*(80/9)*PI*$Hv;    //(db/m)
$alphaaniso=substr($alphaaniso,0,5);

          //calc. of total scattering loss
$totalpha=$alphaiso1+$alphaaniso;
```

```
$talpha[$i][$k]=$totalpha;

fwrite($fp,"<?php");
fwrite($fp," ");
fwrite($fp,"$");
fwrite($fp,"_");
fwrite($fp,$i);
fwrite($fp,$k);
fwrite($fp,"=");
fwrite($fp,$talpha[$i][$k]);
fwrite($fp,";");
fwrite($fp,"?>");

    $dizi2[$i]["l"]=$dizi2[$i]["l"]+100*1e-7;

          } //end of lambda loop

  //echo $alphaiso1;
  }
 //print_r($talpha);

fclose($fp);
 }  //end of if


        //calc. for all (end)

else {  //$all != 1
?>

<br>
<?
        //calc. of isotropic scattering loss 1
$Vv1=(PI*PI*($index2-1)*($index2-
1)*($index2+2)*($index2+2)*BOLTZMANN*$temp*$beta)/(9*$lambda4);
$alphaiso1=4.342e3*(8/3)*PI*$Vv1;    //(db/m)
$alphaiso1=substr($alphaiso1,0,5);
//print("<big><b>...Polarized Scattering Intensity=</b></big>$Vv1\n");
//print("<big><b>...Isotropic Scattering Loss=</b></big>$alphaiso1\n");
?>

<?
        //calc. of anisotropic scattering loss
$Hv=(16*PI*PI*($index2+2)*($index2+2)*$N*$deltasq)/(135*$lambda4);
$alphaaniso=4.342e3*(80/9)*PI*$Hv;    //(db/m)
```

```
$alphaaniso=substr($alphaaniso,0,5);
//print("<big><b>...Depolarized Scattering Intensity=</b></big>$Hv\n");
//print("<big><b>...Anisotropic Scattering Loss=</b></big>$alphaaniso\n");
?>
<?
	//calc. of total scattering loss
$totalpha=$alphaiso1+$alphaaniso;
?>

<?
	//calc. of isotropic scattering loss 1 fom eq.7
$alphaiso17=(1.0e-20*($index2-1)*($index2-1)*($index2+2)*($index2+2))/$lambda4;
$alphaiso17=substr($alphaiso17,0,5);
?>


<?
	//calc. of anisotropic scattering loss 1 fom eq.10
$alphaaniso10=(8.5e-19*($index2+2)*($index2+2)*$rho*((5*$P*$P)+0.3))/$lambda4;
$alphaaniso10=substr($alphaaniso10,0,5);
?>

<?
	//calc. of total scattering loss empirically
$totalphaemp=$alphaiso17+$alphaaniso10;
?>

<?print("<big><b>RESULTS for: $polymer</b></big>");?>
<br>
<br>

<?
	//result table
print("<table border=5>
<tr>
<td align=center><i>&#955 (nm)</i> </td>
<td align=center><i>n</i> </td>
<td align=center><i>T (<sup><small>0</small></sup>C)</i> </td>
<td align=center><i>&#946 (cm<sup><small>2</small></sup>/dyn)</i> </td>
<td align=center><i>N (cm<sup><small>-3</small></sup>)</i> </td>
<td align=center><i>&#948 <sup><small>2</small></sup>
(cm<sup><small>6</small></sup>)</i> </td>
<td align=center><i>&#961 / M (mol / cm<sup><small>3</small></sup>)</i> </td>
<td align=center><i>p</i> </td>
<td align=center><i>k (erg / K)</i> </td>
```

```
<td align=center><i>N<small><sub>0</sub></small></i> </td>
</tr>
<tr>
<td align=center>633</td>
<td align=center>$index</td>
<td align=center>$t</td>
<td align=center>$beta</td>
<td align=center>$N</td>
<td align=center>$deltasq</td>
<td align=center>$rho</td>
<td align=center>$P</td>
<td align=center>$B</td>
<td align=center>$A</td>
</tr>
</table>\n");
?>
<br>

<?
print("<table border=5>
<tr>
<td align=center><i>&#945 <small><sub>iso</sub><sup>1</sup></small> (db /
m)</i> </td>
<td align=center><i>&#945 <small><sub>iso</sub><sup>1</sup></small> (db / m)
empirical</i> </td>
<td align=center><i>&#945 <small><sub>aniso</sub></small>  (db / m)</i> </td>
<td align=center><i>&#945 <small><sub>aniso</sub></small> (db / m) empirical</i>
</td>
<td align=center><i>&#945 <small><sub>t</sub></small> (db / m)</i></td>
<td align=center><i>&#945 <small><sub>t</sub></small> (db / m) emp.</i></td>
</tr>
<tr>
<td bgcolor=#FF0000 align=center>$alphaiso1</td>
<td align=center>$alphaiso17</td>
<td bgcolor=#FF0000 align=center>$alphaaniso</td>
<td align=center>$alphaaniso10</td>
<td bgcolor=#FF0000 align=center>$totalpha</td>
<td align=center>$totalphaemp</td>
</tr>
</table>\n");
?>


<br>
```

```
<?
  if ($all == "PMMA")
{
        //PMMA isothermal comp. table
print("<table border=5>

<tr>
      <td><i>T (<sup><small>0</small></sup>C)</i></td>
      <td>20</td>
      <td>60</td>
      <td>100</td>
      <td>109.3</td>
      <td>119.8</td>
      <td>129.7</td>
      <td>150</td>
      <td>200</td>
</tr>
<tr>
      <td><i>&#946 (cm<sup><small>2</small></sup>/dyn)</i>*10<sup><small>-
11</small></sup></td>
      <td>2.45</td>
      <td>2.90</td>
      <td>3.55</td>
      <td>3.90</td>
      <td>5.00</td>
      <td>5.30</td>
      <td>5.61</td>
      <td>6.44</td>
</tr>
</table>
\n");
?>
<?

$beta1 = array(
        array("t"=>20,"b"=>2.45e-11),
                array("t"=>60,"b"=>2.90e-11),
        array("t"=>100,"b"=>3.55e-11),
                array("t"=>109.3,"b"=>3.90e-11),
        array("t"=>119.8,"b"=>5.00e-11),
                array("t"=>129.7,"b"=>5.30e-11),
        array("t"=>150,"b"=>5.61e-11),
                array("t"=>200,"b"=>6.44e-11),
                );
```

```
	$fp=fopen("variable_pmma_beta.php","w");
	for ($j = 0; $j <=7; $j++)    //loop pmma beta
		{
$Vv1=0;
$alphaiso1=0;

		//calc. of isotropic scattering loss 1
$Vv1=(PI*PI*($index2-1)*($index2-
1)*($index2+2)*($index2+2)*BOLTZMANN*$beta1[$j]["t"]*$beta1[$j]["b"])/(9*$lam
bda4);
$alphaiso1=4.342e3*(8/3)*PI*$Vv1;    //(db/m)
$alphaiso1=substr($alphaiso1,0,5);
$beta_result[$j][0]=$alphaiso1;

fwrite($fp,"<?php");
fwrite($fp," ");
fwrite($fp,"$");
fwrite($fp,"_");
fwrite($fp,$j);
fwrite($fp,0);
fwrite($fp,"=");
fwrite($fp,$beta_result[$j][0]);
fwrite($fp,";");

fwrite($fp," ");
fwrite($fp,"$");
fwrite($fp,"b");
fwrite($fp,$j);
fwrite($fp,"=");
fwrite($fp,$beta1[$j]["b"]*1e11);
fwrite($fp,";");
fwrite($fp,"?>");

	}    //end of loop pmma beta
fclose($fp);
//print_r($beta_result);
?>

<html>
<head>
</head>

<body>
<form NAME="pmmagraphbutton"  action="pmma_graph.php" method="post">
<CENTER><input type="submit" name="submit" value=" GRAPH "></CENTER>
```

```
</form>
</body>
</html>
<?}?>

<?
}
?>

<?php
  if ($all == 1)
{ ?>
<html>
<head>
</head>

<body>
<form NAME="allgraphbutton"  action="all_graph.php" method="post">
<CENTER><input type="submit" name="submit" value="              GRAPH
"></CENTER>
</form>
</body>
</html>

<?}?>

<?php
  if ($all != 1 or $all !="PMMA")
{ ?>
<html>
<head>
</head>

<body>
<form NAME="backbutton">
<CENTER><input type="button" value="BACK"
onClick="history.back()"></CENTER>
</form>
</body>
</html>

<?}?>
```

Code of the Graph of Isotropic Scattering Loss Versus Isothermal Compressibility for PMMA

```
<?php
include "variable_pmma_beta.php";
Header("Content-type: image/jpeg");

$alphaiso1[0][0]=$_00;
$alphaiso1[1][0]=$_10;
$alphaiso1[2][0]=$_20;
$alphaiso1[3][0]=$_30;
$alphaiso1[4][0]=$_40;
$alphaiso1[5][0]=$_50;
$alphaiso1[6][0]=$_60;
$alphaiso1[7][0]=$_70;

$beta = array ($b0,$b1,$b2,$b3,$b4,$b5,$b6,$b7);

$resim = ImageCreate(675,420);
$zemin = ImageColorAllocate($resim,200,200,180);
$black = ImageColorAllocate($resim,0,0,0);

$x=50;
$y=30;
ImageLine($resim,$x,$y-20,$x,$y+300,$black);
ImageLine($resim,$x-20,$y+280,$x+600,$y+280,$black);

ImageLine($resim,$x-20+80 ,$y+275,$x-20+80 ,$y+285,$black);
ImageLine($resim,$x-20+160,$y+275,$x-20+160,$y+285,$black);
ImageLine($resim,$x-20+240,$y+275,$x-20+240,$y+285,$black);
ImageLine($resim,$x-20+320,$y+275,$x-20+320,$y+285,$black);
ImageLine($resim,$x-20+400,$y+275,$x-20+400,$y+285,$black);
ImageLine($resim,$x-20+480,$y+275,$x-20+480,$y+285,$black);
ImageLine($resim,$x-20+560,$y+275,$x-20+560,$y+285,$black);

ImageLine($resim,$x-5,$y+280-70,$x+5,$y+280-70,$black);
ImageLine($resim,$x-5,$y+280-140,$x+5,$y+280-140,$black);
ImageLine($resim,$x-5,$y+280-210,$x+5,$y+280-210,$black);
ImageLine($resim,$x-5,$y+280-280,$x+5,$y+280-280,$black);


ImageArc($resim,$x-20+80+$beta[0]+36,310-$alphaiso1[0][0]*100-
9.2,10,10,0,360,$black);
```

```
ImageArc($resim,$x-20+80+$beta[1]+72,310-23.3-$alphaiso1[1][0]*100-
11.6,10,10,0,360,$black);
ImageArc($resim,$x-20+240+$beta[2]+44,310-70-$alphaiso1[2][0]*100-
4.66,10,10,0,360,$black);
ImageArc($resim,$x-20+240+$beta[3]+72,310-70-$alphaiso1[3][0]*100-
18.6,10,10,0,360,$black);
ImageArc($resim,$x-20+400+$beta[4],310-116.6-$alphaiso1[4][0]*100-
9.32,10,10,0,360,$black);
ImageArc($resim,$x-20+400+$beta[5]+24,310-140-$alphaiso1[5][0]*100-
4.66,10,10,0,360,$black);
ImageArc($resim,$x-20+400+$beta[6]+48.8,310-166.6-
$alphaiso1[6][0]*100,10,10,0,360,$black);
ImageArc($resim,$x-20+480+$beta[7]+35.2,310-256.6-$alphaiso1[7][0]*100-
16,10,10,0,360,$black);

$font=8;

$text= "3";
ImageString($resim,$font,$x-15,$y+280-78,$text,$black);

$text= "6";
ImageString($resim,$font,$x-15,$y+280-148,$text,$black);

$text= "9";
ImageString($resim,$font,$x-15,$y+280-218,$text,$black);

$text= "12";
ImageString($resim,$font,$x-23,$y+280-288,$text,$black);

$text= "1";
ImageString($resim,$font,$x-20+77,$y+280+5,$text,$black);

$text= "2";
ImageString($resim,$font,$x-20+157,$y+280+5,$text,$black);

$text= "3";
ImageString($resim,$font,$x-20+237,$y+280+5,$text,$black);

$text= "4";
ImageString($resim,$font,$x-20+317,$y+280+5,$text,$black);

$text= "5";
ImageString($resim,$font,$x-20+397,$y+280+5,$text,$black);

$text= "6";
```

```
ImageString($resim,$font,$x-20+477,$y+280+5,$text,$black);

$text= "7";
ImageString($resim,$font,$x-20+557,$y+280+5,$text,$black);
$text= "Isothermal Compressibility (cm2/dyn)";
ImageString($resim,$font,$x+140,$y+310,$text,$black);

$text= "Iso. Scattering Loss (db/m)*E-2";
ImageStringUp($resim,$font,$x-40,$y+270,$text,$black);

$text=": Isotropic scattering loss for PMMA";
ImageArc($resim,$x-10,$y+350,10,10,0,360,$black);
ImageString($resim,$font,$x+5,$y+350-$font,$text,$black);

ImageJPEG($resim);
ImageDestroy($resim);
?>
```

Code of the Graph of Total Attenuation Versus Wavelength

```
<?php
include "variable_all.php";
Header("Content-type: image/jpeg");

$talpha=array(
        array($_00,$_01,$_02,$_03,$_04,$_05),
                array($_10,$_11,$_12,$_13,$_14,$_15),
        array($_20,$_21,$_22,$_23,$_24,$_25),
                array($_30,$_31,$_32,$_33,$_34,$_35),
        array($_40,$_41,$_42,$_43,$_44,$_45),
                array($_50,$_51,$_52,$_53,$_54,$_55),
                );

$resim = ImageCreate(675,420);
$zemin = ImageColorAllocate($resim,200,200,180);
$red = ImageColorAllocate($resim,255,0,0);
$blue = ImageColorAllocate($resim,0,0,255);
$black = ImageColorAllocate($resim,0,0,0);
$s = ImageColorAllocate($resim,253,41,211);

$x=50;
$y=30;
ImageLine($resim,$x,$y-20,$x,$y+300,$black);
ImageLine($resim,$x-20,$y+280,$x+600,$y+280,$black);

ImageLine($resim,$x-20+100,$y+275,$x-20+100,$y+285,$black);
ImageLine($resim,$x-20+200,$y+275,$x-20+200,$y+285,$black);
ImageLine($resim,$x-20+300,$y+275,$x-20+300,$y+285,$black);
ImageLine($resim,$x-20+400,$y+275,$x-20+400,$y+285,$black);
ImageLine($resim,$x-20+500,$y+275,$x-20+500,$y+285,$black);
ImageLine($resim,$x-20+600,$y+275,$x-20+600,$y+285,$black);

ImageLine($resim,$x-5,$y+280-95,$x+5,$y+280-95,$black);
ImageLine($resim,$x-5,$y+280-185,$x+5,$y+280-185,$black);
ImageLine($resim,$x-5,$y+280-275,$x+5,$y+280-275,$black);

   //PMMA
ImageArc($resim,$x-20+100,310-$talpha[0][0]*100,10,10,0,360,$black);
ImageArc($resim,$x-20+200,310-$talpha[0][1]*100,10,10,0,360,$black);
ImageArc($resim,$x-20+300,310-$talpha[0][2]*100,10,10,0,360,$black);
ImageArc($resim,$x-20+400,310-$talpha[0][3]*100,10,10,0,360,$black);
ImageArc($resim,$x-20+500,310-$talpha[0][4]*100,10,10,0,360,$black);
ImageArc($resim,$x-20+600,310-$talpha[0][5]*100,10,10,0,360,$black);
```

```
ImageFill($resim,$x-20+100,310-$talpha[0][0]*100,$black);
ImageFill($resim,$x-20+200,310-$talpha[0][1]*100,$black);
ImageFill($resim,$x-20+300,310-$talpha[0][2]*100,$black);
ImageFill($resim,$x-19+400,310-$talpha[0][3]*100,$black);
ImageFill($resim,$x-19+500,310-$talpha[0][4]*100,$black);
ImageFill($resim,$x-21+600,310-$talpha[0][5]*100,$black);


   //PSt
ImageRectangle($resim,$x-20+100,310-$talpha[1][0]*100,$x-20+100+10,310-
$talpha[1][0]*100+10,$black);
ImageRectangle($resim,$x-20+200,310-$talpha[1][1]*100,$x-20+200+10,310-
$talpha[1][1]*100+10,$black);
ImageRectangle($resim,$x-20+300,310-$talpha[1][2]*100,$x-20+300+10,310-
$talpha[1][2]*100+10,$black);
ImageRectangle($resim,$x-20+400,310-$talpha[1][3]*100,$x-20+400+10,310-
$talpha[1][3]*100+10,$black);
ImageRectangle($resim,$x-20+500,310-$talpha[1][4]*100,$x-20+500+10,310-
$talpha[1][4]*100+10,$black);
ImageRectangle($resim,$x-20+600,310-$talpha[1][5]*100,$x-20+600+10,310-
$talpha[1][5]*100+10,$black);

   //PC
ImageFilledRectangle($resim,$x-20+100,310-$talpha[2][0]*100,$x-20+100+10,310-
$talpha[2][0]*100+10,$black);
ImageFilledRectangle($resim,$x-20+200,310-$talpha[2][1]*100,$x-20+200+10,310-
$talpha[2][1]*100+10,$black);
ImageFilledRectangle($resim,$x-20+300,310-$talpha[2][2]*100,$x-20+300+10,310-
$talpha[2][2]*100+10,$black);
ImageFilledRectangle($resim,$x-20+400,310-$talpha[2][3]*100,$x-20+400+10,310-
$talpha[2][3]*100+10,$black);
ImageFilledRectangle($resim,$x-20+500,310-$talpha[2][4]*100,$x-20+500+10,310-
$talpha[2][4]*100+10,$black);
ImageFilledRectangle($resim,$x-20+600,310-$talpha[2][5]*100,$x-20+600+10,310-
$talpha[2][5]*100+10,$black);

   //PAr
ImageArc($resim,$x-20+100,310-$talpha[3][0]*100,10,7,0,360,$black);
ImageArc($resim,$x-20+200,310-$talpha[3][1]*100,10,7,0,360,$black);
ImageArc($resim,$x-20+300,310-$talpha[3][2]*100,10,7,0,360,$black);
ImageArc($resim,$x-20+400,310-$talpha[3][3]*100,10,7,0,360,$black);
ImageArc($resim,$x-20+500,310-$talpha[3][4]*100,10,7,0,360,$black);
ImageArc($resim,$x-20+600,310-$talpha[3][5]*100,10,7,0,360,$black);
```

```
   //PSF
ImageArc($resim,$x-20+100,310-$talpha[4][0]*100,7,10,0,360,$black);
ImageArc($resim,$x-20+200,310-$talpha[4][1]*100,7,10,0,360,$black);
ImageArc($resim,$x-20+300,310-$talpha[4][2]*100,7,10,0,360,$black);
ImageArc($resim,$x-20+400,310-$talpha[4][3]*100,7,10,0,360,$black);
ImageArc($resim,$x-20+500,310-$talpha[4][4]*100,7,10,0,360,$black);
ImageArc($resim,$x-20+600,310-$talpha[4][5]*100,7,10,0,360,$black);

   //PES
ImageArc($resim,$x-20+100,310-$talpha[5][0]*100,10,10,0,360,$black);
ImageArc($resim,$x-20+200,310-$talpha[5][1]*100,10,10,0,360,$black);
ImageArc($resim,$x-20+300,310-$talpha[5][2]*100,10,10,0,360,$black);
ImageArc($resim,$x-20+400,310-$talpha[5][3]*100,10,10,0,360,$black);
ImageArc($resim,$x-20+500,310-$talpha[5][4]*100,10,10,0,360,$black);
ImageArc($resim,$x-20+600,310-$talpha[5][5]*100,10,10,0,360,$black);



$font=8;

$text=": PMMA";
ImageArc($resim,$x-10,$y+350,10,10,0,360,$black);
ImageFill($resim,$x-10,$y+350,$black);
ImageString($resim,$font,$x+5,$y+350-$font,$text,$black);

$text=": PSt";
ImageRectangle($resim,$x-15,$y+365,$x-5,$y+375,$black);
ImageString($resim,$font,$x+5,$y+370-$font,$text,$black);

$text=": PC";
ImageFilledRectangle($resim,$x+150,$y+345,$x+160,$y+355,$black);
ImageString($resim,$font,$x+170,$y+350-$font,$text,$black);

$text=": PAr";
ImageArc($resim,$x+155,$y+370,10,7,0,360,$black);
ImageString($resim,$font,$x+170,$y+370-$font,$text,$black);

$text=": PSF";
ImageArc($resim,$x+300,$y+350,7,10,0,360,$black);
ImageString($resim,$font,$x+320,$y+350-$font,$text,$black);

$text=": PES";
ImageArc($resim,$x+300,$y+370,10,10,0,360,$black);
ImageString($resim,$font,$x+320,$y+370-$font,$text,$black);
```

```
$text= "Attenuation (db/m)";
ImageStringUp($resim,$font,$x-40,$y+200,$text,$black);

$text= "Wavelength (cm)";
ImageString($resim,$font,$x+250,$y+310,$text,$black);

$text= "1";
ImageString($resim,$font,$x-15,$y+280-103,$text,$black);

$text= "2";
ImageString($resim,$font,$x-15,$y+280-193,$text,$black);

$text= "3";
ImageString($resim,$font,$x-15,$y+280-283,$text,$black);

$text= "400";
ImageString($resim,$font,$x-20+87,$y+280+5,$text,$black);

$text= "500";
ImageString($resim,$font,$x-20+187,$y+280+5,$text,$black);

$text= "600";
ImageString($resim,$font,$x-20+287,$y+280+5,$text,$black);

$text= "700";
ImageString($resim,$font,$x-20+387,$y+280+5,$text,$black);

$text= "800";
ImageString($resim,$font,$x-20+487,$y+280+5,$text,$black);

$text= "900";
ImageString($resim,$font,$x-20+587,$y+280+5,$text,$black);

ImageJPEG($resim);
ImageDestroy($resim);
?
```

APPENDIX-B

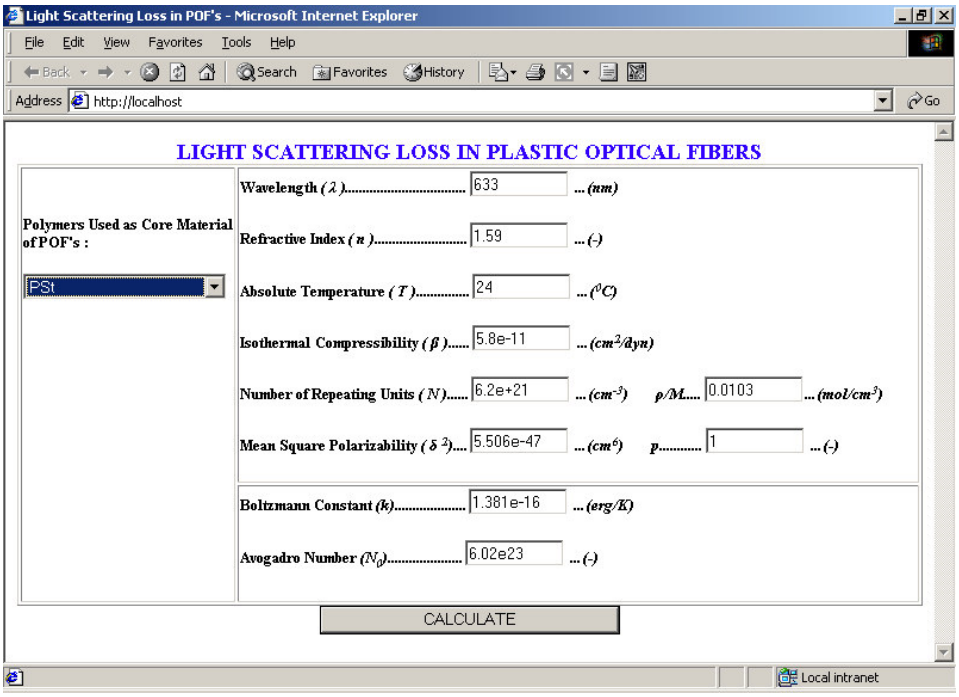

Figure App.B.1 Data screen used in calculation of PSt.

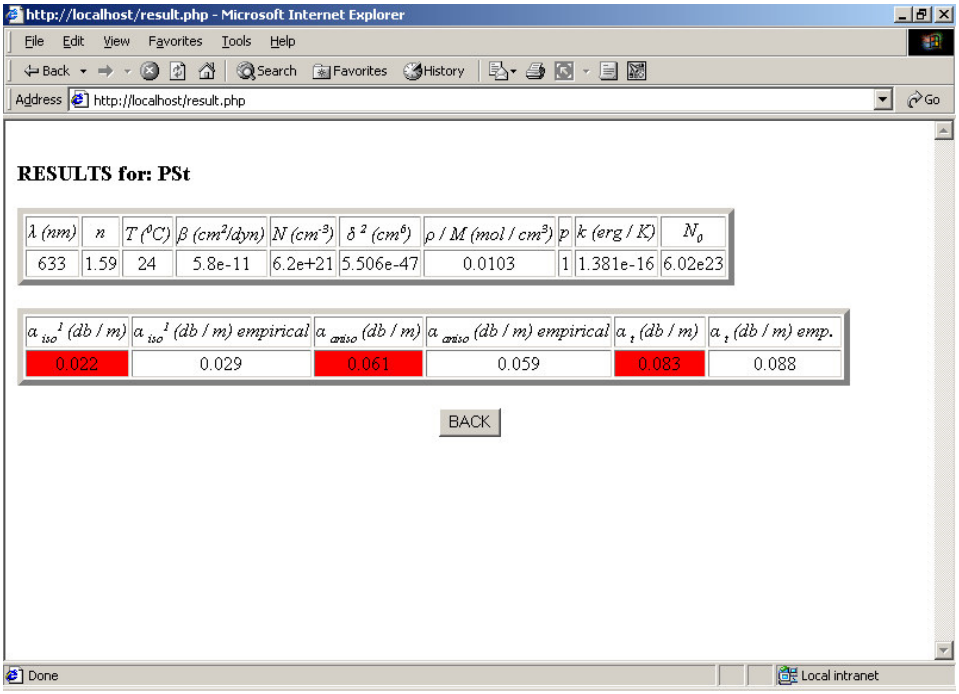

Figure App.B.2 The outputs of results after the calculation for PSt.

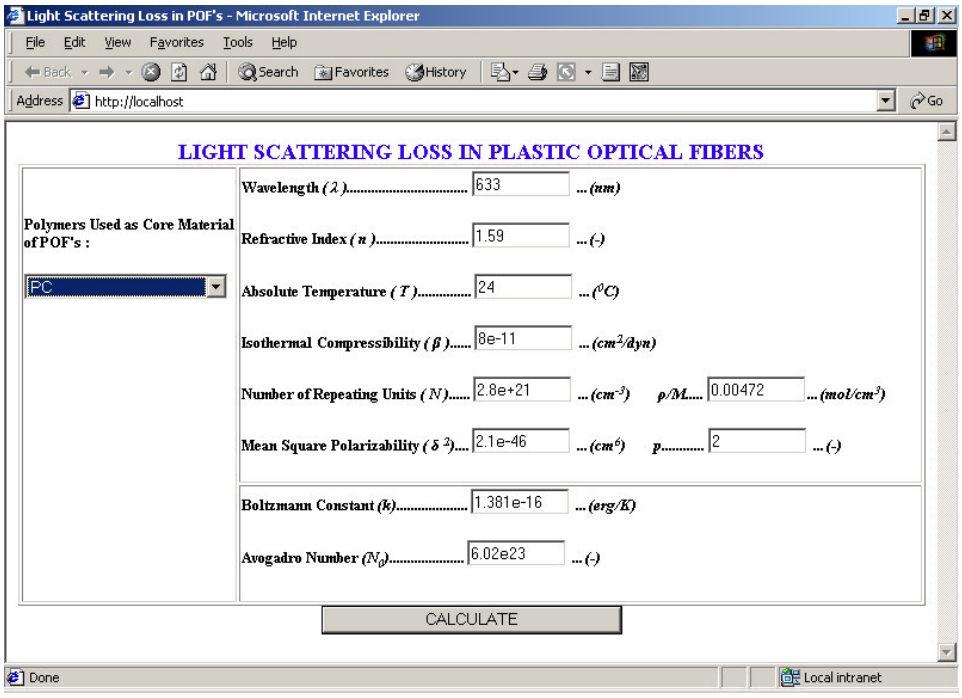

Figure App.B.3 Data screen used in calculation of PC.

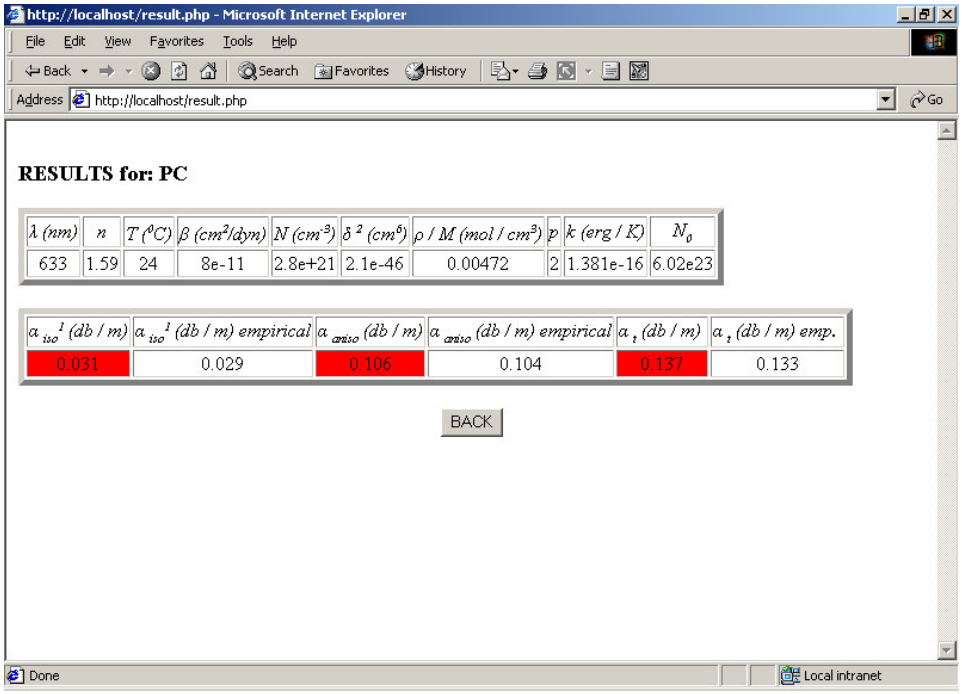

Figure App.B.4 The outputs of results after the calculation for PC.

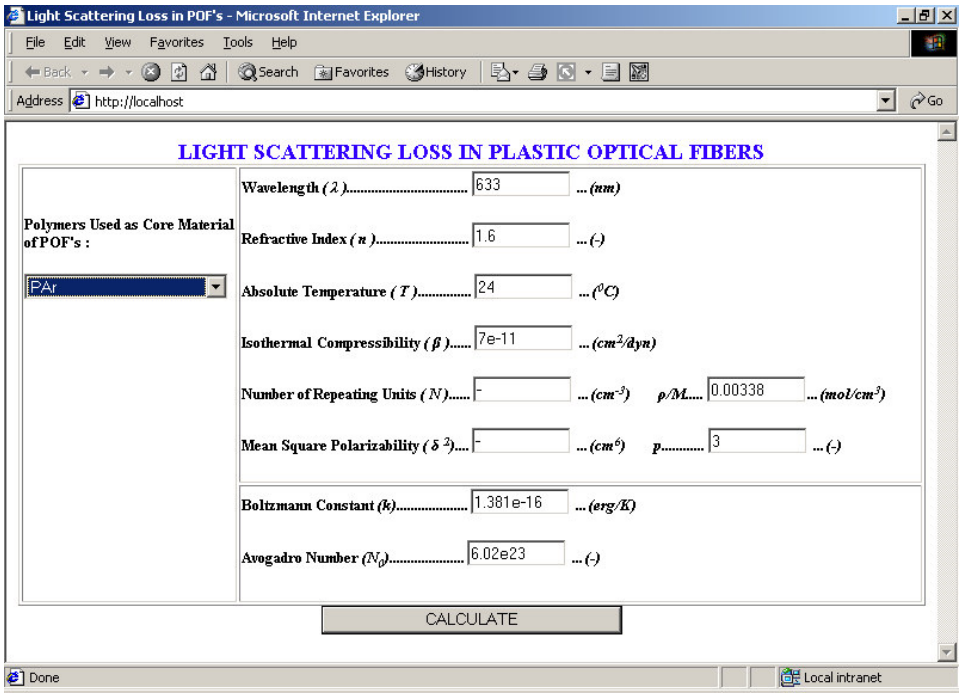

Figure App.B.5 Data screen used in calculation of PAr.

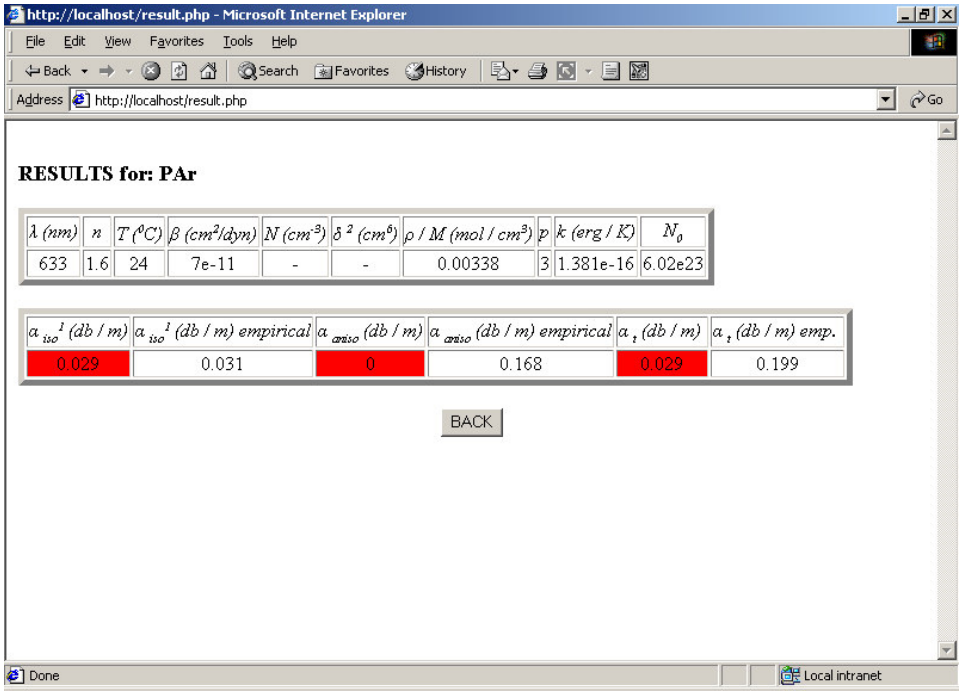

Figure App.B.6 The outputs of results after the calculation for PAr.

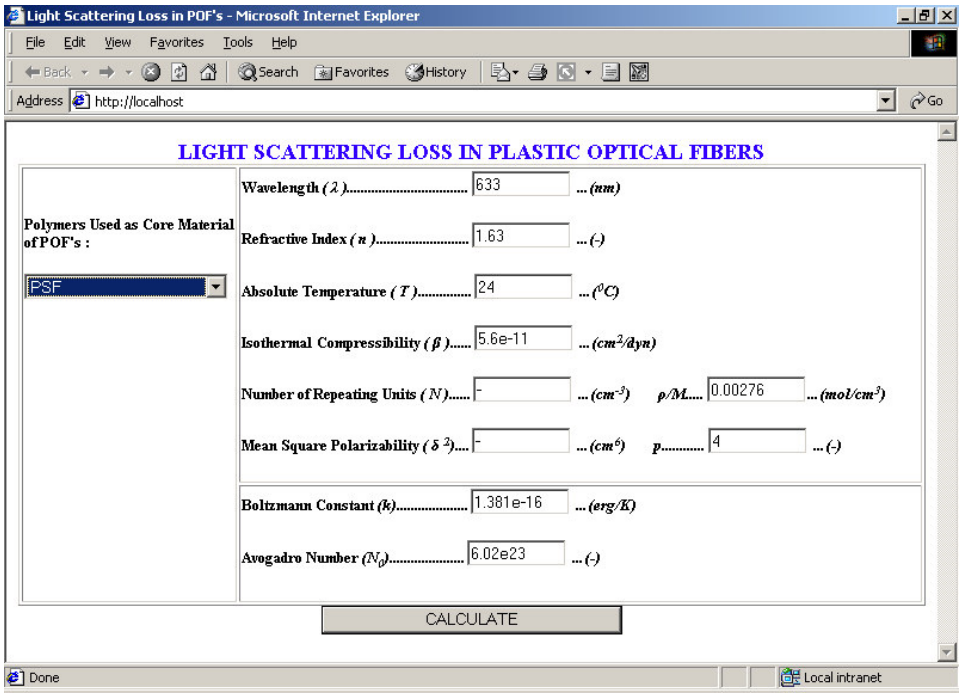

Figure App.B.7 Data screen used in calculation of PSF.

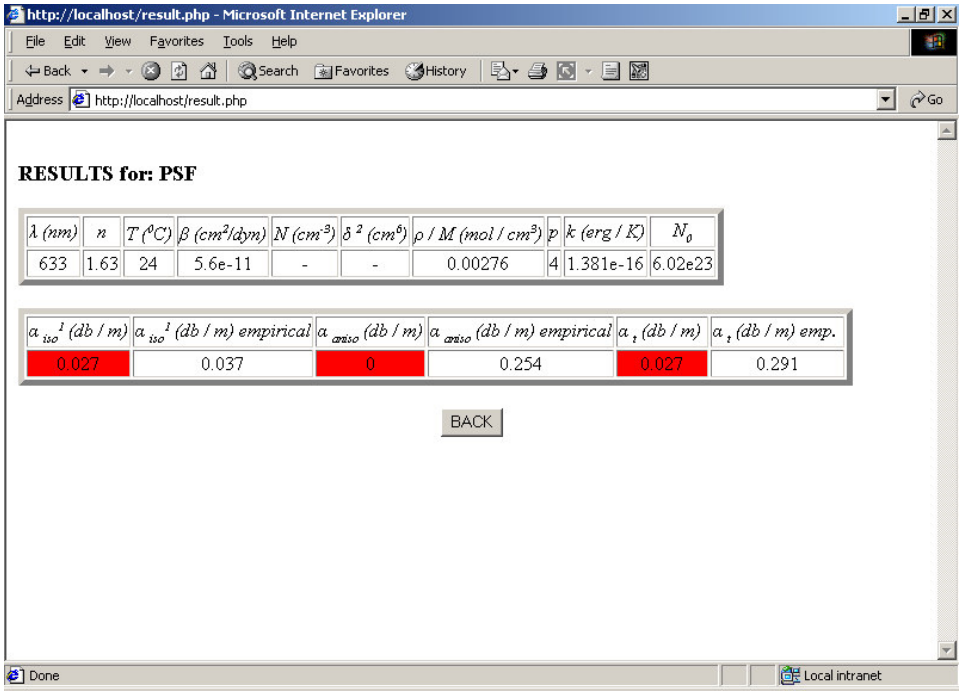

Figure App.B.8 The outputs of results after the calculation for PSF.

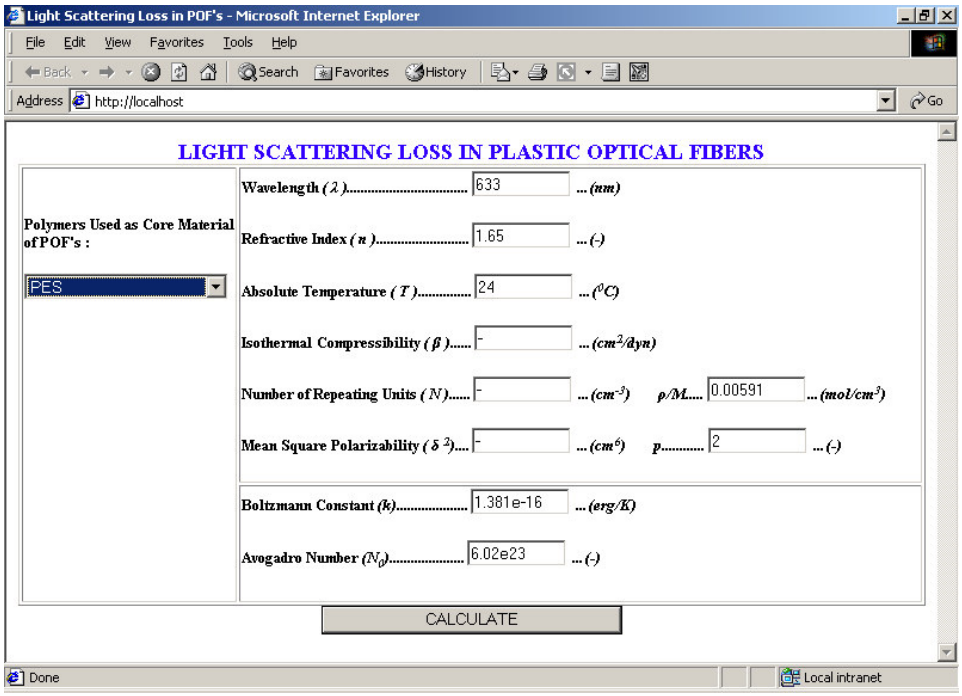

Figure App.B.9 Data screen used in calculation of PES.

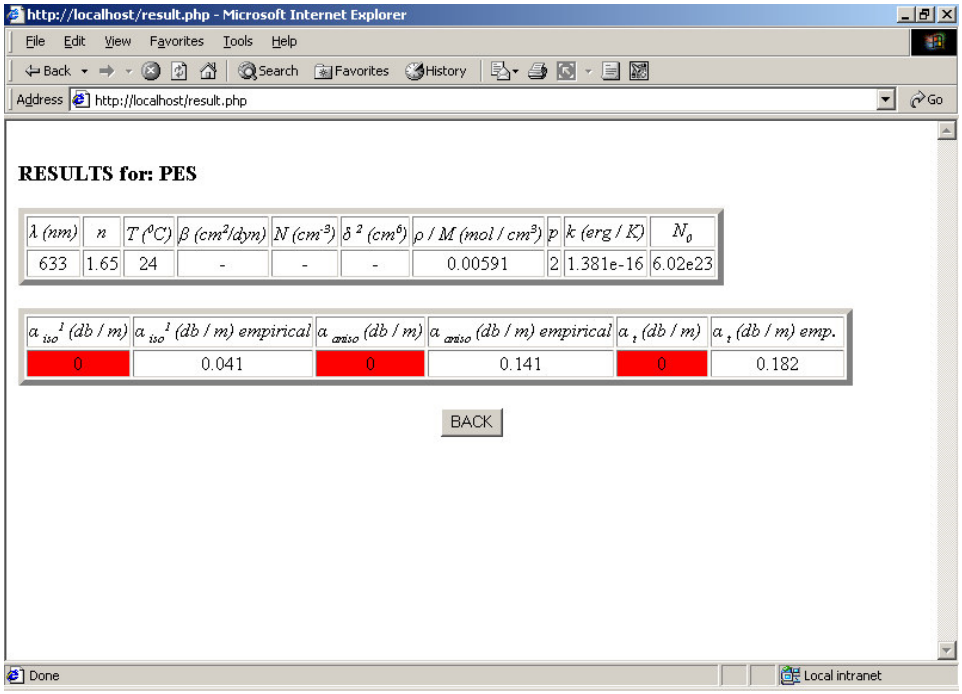

Figure App.B.10 The outputs of results after the calculation for PES.